

## **Improved chronic wound therapy: surface charged deformable liposomes for dermal delivery of curcumin**

**Eivind Gagnat**

*Master's thesis in Pharmacy, May 2018*

*Drug Transport and Delivery Research Group*

Supervisors

PhD student Selenia Ternullo

Professor Nataša Škalko-Basnet



## Acknowledgements

This study was conducted at the Drug Transport and Delivery Group, Department of Pharmacy, UiT – The Arctic University of Norway from September 2017 to May 2018.

First, I want to express my greatest gratitude towards my supervisors Professor Nataša Škalko-Basnet and PhD student Selenia Ternullo for the opportunity to write my master thesis at the Drug Transport and Delivery Group. Especially, I would thank Selenia Ternullo for having the patience to guide me in the lab and sharing your knowledge. It has been an honor to work with you, and I wish you the best with your PhD.

For the help with the anti-inflammatory experiments in this study, I would like to thank Professor II Purusotam Basnet.

I would also give my appreciation to all of the other people attending the lab in the Drug Transport and Delivery Group, in particular Sabrin and Mia at the Franz diffusion lab for the fun experiences and support during long days at the lab, and Laura for the great cooperation and shared frustrations over curcumin. In addition, I will thank the others at “the office”, and Betty for the good times.

A Special thanks to my boyfriend Mats Andreas for supporting me through this period and bringing me sweet music every day ♥ love you big time! Also, Monika, Rune, Karin and Arnfinn for the frequent dinners, Camilla for providing me with beer when in Kolbotn, and my two older sisters for bullying me when I was young, making me tough enough to handle life.

My final thoughts go to my parents and family at Gagnat, thank you for all support in life, and during the five years of studying. I could never have done this without you.



## Abstract

Chronic wounds are today representing a major challenge in global healthcare due the difficulty to treat as well as the costs for the society. Therefore, improving chronic wound therapy is an urgent need. Curcumin, a polyphenol compound, has shown to have potential in wound therapy due to its anti-inflammatory, anti-infectious and anti-oxidant properties. However, the poor water solubility, low bioavailability and rapid degradation represent major challenges in optimizing formulation of curcumin for delivery.

The aim of this study was to develop deformable liposomes to improve dermal delivery of curcumin. The liposomes were prepared by thin film hydration method and extruded through polycarbonate membranes to obtain the desired vesicle size. The deformable liposomes were characterized for the size, polydispersity, surface charge and entrapment efficiency. *In vitro* and *ex vivo* curcumin release from the deformable liposomes were examined using Franz diffusion cells with cellophane and full-thickness human skin as membranes, respectively. Anti-inflammatory activity, anti-bacterial activity and cell proliferation studies of the different deformable liposomes were assessed to confirm the potential in treatment of chronic wounds.

All deformable liposomes were in a size range between 200 and 300 nm as we aimed at the start of this study, exhibiting a relatively homogenous size distribution. The zeta potential was corresponding to the liposomal composition used in the preparation of liposomes. Anionic deformable liposomes (ADL) showed the highest entrapment efficiency (0.11 mg curcumin/mg lipid) compared to cationic deformable liposomes (CDL) and neutral deformable liposomes (NDL), and, in addition, the highest amount of penetrated curcumin through the full thickness human skin. A concentration-dependent effect was observed regarding the anti-inflammatory activity and cell proliferation assay, where CDL and NDL were shown to exhibit the strongest effect. CDL showed the strongest anti-bacterial activity against *S. aureus* and *S. pyogenes* as well.

In conclusion, ADL penetrated the skin to a greatest extent. On the other hand, CDL assured desirable sustained release in addition to the strongest anti-bacterial activity, both features very much favourable regarding wound therapy. Incorporation of curcumin in deformable liposomes enhanced its anti-inflammatory effect and cell proliferation in comparison to free curcumin.

Keywords: Chronic wounds, deformable liposomes, curcumin, human skin.

## Abstract (Norwegian)

Kroniske sår representerer i dag en stor utfordring for det globale helsevesen på grunn av komplisert behandling og kostnader for samfunnet. Derfor er viktigheten av forbedring et akutt behov. Kurkumin, en polyfenol-forbindelse, har vist potensiale i sårbehandling med bakgrunn i dets antiinflammatoriske, antibakterielle og antioksidant egenskaper. Derimot utgjør den lave vannløseligheten, lave biotilgjengeligheten og rask degradering av virkestoffet en utfordring i å optimalisere formuleringer for administrasjon.

Målet i denne studien var å utvikle deformerbare liposomer for forbedring av dermal administrasjon av kurkumin. Liposomene ble fremstilt i henhold til «thin film hydration»-metoden og ekstrudert gjennom polykarbonatmembraner for å oppnå den ønskede vesikkelstørrelse. De deformerbare liposomene ble karakterisert med tanke på størrelse, størrelsesfordeling, overflateladning og mengde kurkumin inkorporert i liposomene. *In vitro* og *ex vivo* frigjøring av kurkumin fra de deformerbare liposomene ble undersøkt ved bruk av Franz diffusjon celler, med cellofan og menneskehud i full tykkelse brukt som membraner. Antiinflammatorisk aktivitet, antibakteriell aktivitet og celleprolifisering ble undersøkt for å bekrefte potensialet for behandling av kroniske sår.

Alle de deformerbare liposomer hadde en størrelse mellom 200 og 300 nm som var målet fra starten i denne studien, og viste en homogen størrelsesfordeling. Zetapotensiale samsvarte med liposomal komposisjon brukt i fremstillingen av liposomene. Anioniske deformerbare liposomer (ADL) viste høyest inkorporering av kurkumin (0.11 mg kurkumin/mg lipid) sammenlignet med kationiske deformerbare liposomer (CDL) og nøytrale deformerbare liposomer (NDL), og viste også størst penetrasjon av kurkumin gjennom menneskehud i full tykkelse. Vedrørende antiinflammatorisk aktivitet og celleprolifisering ble det observert en konsentrasjonsavhengig effekt hvor henholdsvis CDL og NDL viste best effekt. CDL viste størst antibakteriell aktivitet mot *S. aureus* og *S. pyogenes*.

Til konklusjon viste forsøkene at ADL penetrerer menneskehud best. CDL viste en ønsket forlenget frigjøringsprofil i tillegg til best antibakteriell effekt, begge gunstige egenskaper i forhold til sårbehandling. Kurkumin inkorporert i deformerbare liposomer økte dets antiinflammatorisk effekt og celleprolifisering sammenlignet med fritt kurkumin.

Nøkkelord: Kroniske sår, deformerbare liposomer, kurkumin, menneskehud

# Table of Contents

Acknowledgements .....	II
Abstract .....	IV
Abstract (Norwegian) .....	V
List of abbreviations .....	1
1 Introduction .....	2
1.1 Skin.....	2
1.1.1 Skin structure.....	2
1.1.2 Skin function .....	3
1.1.3 Skin penetration pathways.....	4
1.2 Wounds.....	5
1.2.1 Wound healing process.....	5
1.2.2 Chronic wounds.....	6
1.2.3 Conventional treatment of chronic wounds.....	7
1.3 Curcumin .....	8
1.3.1 Curcumin in wound healing .....	9
1.4 (Trans)dermal delivery .....	10
1.4.1 Improvement of dermal delivery .....	10
1.5 Nanotechnology.....	11
1.5.1 Conventional liposomes .....	11
1.5.2 Deformable liposomes.....	13
1.5.3 Other liposomes.....	13
1.5.4 Liposomes in wound dressings.....	14
2 Aim of the study .....	15
3 Materials and methods.....	17
3.1 Materials.....	17
3.1.1 Materials used.....	17
3.1.2 Equipment and devices.....	18
3.1.3 Software.....	19
3.2 Methods.....	20
3.2.1 Preparation of phosphate buffer saline (PBS) .....	20
3.2.2 Preparation of conventional liposomes .....	20
3.2.3 Deformable liposomes.....	21
3.2.4 Ethosomes .....	21

3.2.5	Propylene glycol (PG) deformable liposomes.....	22
3.3	Size reduction.....	22
3.3.1	Extrusion.....	22
3.3.2	Sonication.....	23
3.4	Size measurements.....	23
3.5	Zeta potential measurements.....	24
3.6	Curcumin entrapment.....	24
3.7	Quantification of curcumin.....	24
3.8	Phospholipid quantification.....	24
3.9	<i>In vitro</i> curcumin release.....	25
3.10	<i>Ex vivo</i> skin penetration of curcumin.....	26
3.11	Anti-inflammatory potential of liposomal curcumin.....	27
3.12	Anti-bacterial activity.....	28
3.13	<i>In vitro</i> cell toxicity and proliferation assay.....	28
3.14	Stability of liposomes.....	29
3.15	Statistical analysis.....	29
4	Results and discussion.....	30
4.1	Conventional liposomes.....	30
4.2	Deformable liposomes.....	31
4.2.1	Size.....	32
4.2.2	Polydispersity of deformable liposomes.....	33
4.2.3	Surface charge.....	33
4.2.4	Entrapment of curcumin.....	33
4.2.5	Lipid content.....	34
4.3	<i>In vitro</i> curcumin release.....	34
4.4	<i>Ex vivo</i> skin penetration of curcumin.....	36
4.5	Ethosomes/PG deformable liposomes.....	38
4.6	Anti-inflammatory potential of liposomal curcumin.....	39
4.7	Anti-bacterial activity.....	41
4.8	<i>In vitro</i> cell toxicity and proliferation assay.....	42
4.9	Stability of liposomes.....	44
5	Conclusions.....	47
6	Perspectives.....	48
	References.....	49

## List of Tables

<b>Table 1:</b> Composition of the curcumin-loaded deformable liposomes.....	21
<b>Table 2:</b> Cycles of extrusion for the different types of deformable liposomes containing curcumin...	23
<b>Table 3:</b> Characteristics of conventional liposomes containing curcumin (n=3 ± SD).....	30
<b>Table 4:</b> Size of empty conventional liposomes obtained through extrusion and sonication (n=3).....	31
<b>Table 5:</b> Characteristics of the deformable liposomes containing curcumin. The results are expressed as mean ± SD (n=3).....	32
<b>Table 6:</b> Characterization of ethosomes (n=1). .....	39
<b>Table 7:</b> Anti-bacterial effect of different deformable liposomes containing curcumin expressed as bacterial survival in percentage ± SD (n=2). *Significantly lower than control: *p < 0.03, **p < 0.002, ***p < 0.0002, ****p < 0.0001. °Significantly lower than CUR-PG: °p < 0.03, °°p < 0.002, °°°p < 0.0002, °°°°p < 0.0001. ....	42

## List of Figures

<b>Figure 1:</b> The structure of the human skin ( <a href="http://wamc.org/post/vox-pop-medical-monday-dermatology-dr-jerome-hill-52013">http://wamc.org/post/vox-pop-medical-monday-dermatology-dr-jerome-hill-52013</a> ) .....	3
<b>Figure 2:</b> Penetration pathways through the stratum corneum barrier (Dąbrowska et al., 2017) (Copyright© reprinted with permission from RightsLink®). .....	5
<b>Figure 3:</b> Wound healing phases including the involved cells (Li et al., 2007) (Copyright© reprinted with permission from RightsLink®). .....	6
<b>Figure 4:</b> Curcuma longa with its rhizome and powder <a href="http://ottawavalleydogwhisperer.blogspot.no/2012/11/turmeric-and-curcumin-good-for-your.html">http://ottawavalleydogwhisperer.blogspot.no/2012/11/turmeric-and-curcumin-good-for-your.html</a> . ....	8
<b>Figure 5:</b> Chemical structure of the different curcuminoids ( <a href="https://www.spandidos-publications.com/10.3892/mmr.2012.1106">https://www.spandidos-publications.com/10.3892/mmr.2012.1106</a> ) .....	9
<b>Figure 6:</b> Composition of liposome and its lipid bilayer ( <a href="http://fortiferrum.com/liposomal-microencapsulated-iron?lang=en">http://fortiferrum.com/liposomal-microencapsulated-iron?lang=en</a> ) .....	12
<b>Figure 7:</b> Classification of liposomes after size and number of bilayers. LUV – Large uni-lamellar vesicles, SUV – Small uni-lamellar vesicles, MLV – Multi-lamellar vesicles, GUV – Giant uni-lamellar vesicles (Grimaldi et al., 2016) (Copyright© reprinted with permission from RightsLink®).	13
<b>Figure 8:</b> Schematic overview of some of the different types of liposomes and their composition (Hua, 2015) (Copyright© reprinted with permission from RightsLink®). .....	14
<b>Figure 9:</b> Schematic of conventional thin film hydration method ( <a href="http://www.intechopen.com/source/html/44386/media/image7.png">http://www.intechopen.com/source/html/44386/media/image7.png</a> ). .....	20
<b>Figure 10:</b> Schematic view of a Franz cell ( <a href="http://www.permegear.com">www.permegear.com</a> ) .....	26
<b>Figure 11:</b> Penetration profile of curcumin from CDL, ADL and NDL through cellophane membrane. The results are presented as mean ± SD (n=3) .....	35
<b>Figure 12:</b> Penetration profile of curcumin from CDL, ADL and NDL through full-thickness human skin. The results are presented as mean ± SD (n=3). *Significantly higher (*p < 0.05, **p < 0.005) than CDL. ....	37
<b>Figure 13:</b> <i>In vitro</i> and <i>ex vivo</i> penetration (24 hours) of curcumin from deformable liposomes of different surface charge. The results are expressed as mean ± SD (n=3). (CF=Cellophane, HS=Human skin). ....	38
<b>Figure 14:</b> Effect of different formulations on nitric oxide (NO) production in lipopolysaccharide (LPS)-induced macrophages. The results are expressed as absorbance with mean ± SD (n=3). *Significantly lower than control: *p < 0.03, **p < 0.002, ***p < 0.0002, ****p < 0.0001. °Significantly lower than CUR-PG: °p < 0.03, °°p < 0.002, °°°p < 0.0002, °°°°p < 0.0001. ....	40
<b>Figure 15:</b> <i>In vitro</i> proliferation assay. The results are expressed as the mean optical density (O.D.) values ± SD (n=3) measured using CCK-8 colorimetric assay. *Significantly different than control: *p < 0.03, **p < 0.002, ***p 0.0002. °Significantly different than CUR-PG: °p < 0.03, °°p < 0.002, °°°p < 0.0002. ....	43
<b>Figure 16:</b> Size measurements before and after 30 days of storage at 4 °C. ....	44
<b>Figure 17:</b> Zeta potential before and after 30 days of storage at 4 °C. ....	45
<b>Figure 18:</b> Entrapment efficiency expressed as curcumin/ lipid ratio (mg/mg) before and after 30 days of storage at 4 °C. ....	45

## List of abbreviations

ADL	Anionic deformable liposomes
CCK-8	Cell Counting Kit – 8
CDL	Cationic deformable liposomes
CF	Cellophane
CUR	Curcumin
DMDM	Dulbecco's modified eagle's medium
EE	Entrapment Efficiency
HFF	Human Foreskin Fibroblast
HS	Human skin
IVIVC	In-vitro In-vivo correlation
LPS	Lipopolysaccharide
NDL	Neutral deformable liposomes
Nm	Nanometre
NO	Nitric oxide
PBS	Phosphate Buffer Saline
PC	Phosphatidylcholine
PG	Propylene glycol
PI	Polydispersity Index
Rpm	Rotations per minute
Sol	Solution

# 1 Introduction

## 1.1 Skin

### 1.1.1 Skin structure

The skin is the largest organ in the human body, comprising about 15% of an adults' total body weight and providing a large surface area of approximately 2 m<sup>2</sup>. The skin is a multi-layered organ and can be divided into three main layers, namely epidermis, dermis and hypodermis (**Figure 1**) (Ng and Lau, 2015; Lai-Cheong and McGrath, 2017). The outer layer is the epidermis composed of keratinocytes and can be subdivided into four distinct layers representing the state of keratinocyte differentiation. The basal layer, *stratum basale*, holds a single layer of keratinocytes. These keratinocytes undergo differentiation and proliferation while migrating through the different layers of the epidermis (*stratum spinosum*, *stratum granulosum*) ending up as corneocytes (non-living cells) in the outermost layer, *stratum corneum* (Lai-Cheong and McGrath, 2017; van Smeden *et al.*, 2014). Corneocytes are flattened and elongated cells with high content of keratin filament and water surrounded by a lipid matrix and are of great importance for the skin barrier function (Mota *et al.*, 2017; Sala *et al.*, 2018). Beneath the epidermis is the dermis. Depending on the body site, the thickness of the dermis is about 0.5 – 5 mm. The dermis is subdivided in the papillary dermis richly supplied with blood vessels and sensory nerve endings, and the reticular dermis that is connected to the subcutis (Lai-Cheong and McGrath, 2017). The hypodermis (or the subcutis) is the inner layer anchoring the underlying tissue, mainly composed of adipocytes and subcutaneous fat. Embedded in this layer we can find larger lymphatic vessels and blood vessels (Lai-Cheong and McGrath, 2017; Ng and Lau, 2015). Hair follicles and sebaceous glands are embedded in the skin layers where the density of distribution is dependent on the body site (Barry, 1991).

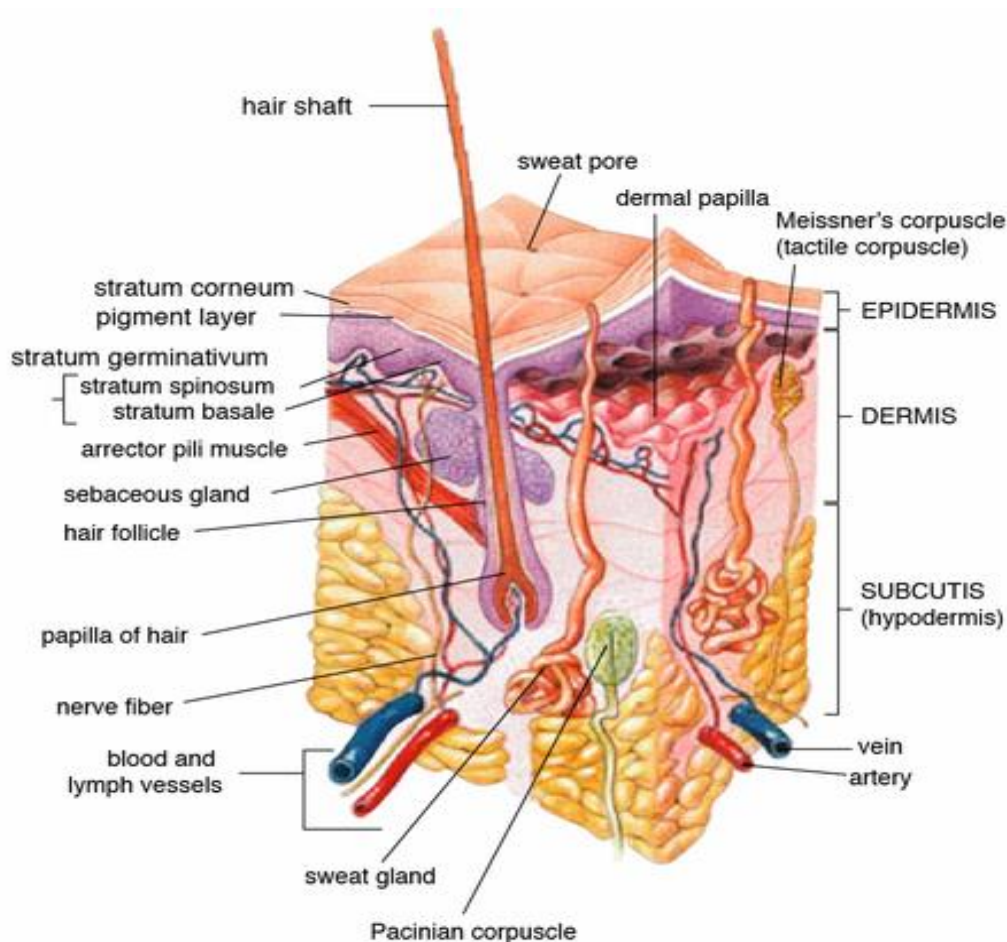


**Figure 1:** The structure of the human skin (<http://wamc.org/post/vox-pop-medical-monday-dermatology-dr-jerome-hill-52013>)

### 1.1.2 Skin function

The skin is a part of the integumentary system and its primary function is to act as a barrier to protect the body against the external non-physiological environment and ensure homeostasis (Banerjee and Sen, 2015; Alexander *et al.*, 2012). This includes prevention of fluid loss and passage of microorganisms and toxic compounds, regulation of body temperature through the sweat and blood flow, peripheral metabolism of hormones and vitamin D synthesis (Menon, 2015; Sala *et al.*, 2018). The *stratum corneum* with its corneocytes is the main responsible for the physical barrier properties exerted by the skin. In addition, the natural acidic pH of the skin (pH = 4-6) epitomizes a chemical barrier, while the immune cells (Langerhans cells and dendritic cells) function as an immunological barrier (Ng and Lau, 2015; Lee and Friedman, 2016). The skin also acts as an alternative administration route for the delivery of active pharmaceutical ingredients. By the skin, the drug can be delivered in the skin layers (dermal

delivery) to exert local effect or the drug can pass through the skin layers and reach the systemic circulation (transdermal delivery) to be absorbed and exert systemic effect (Kotla *et al.*, 2017).

### 1.1.3 Skin penetration pathways

The penetration of substances across the *stratum corneum* barrier of the skin mainly occurs through passive diffusion, and some of the commonly proposed mechanisms are the intercellular, transcellular and transappendageal pathways. These pathways are illustrated in **Figure 2**. The intercellular route is the most dominant pathway and involves transport of substances through the lipid matrix of the *stratum corneum*, and lipophilic substances are more likely to use this pathway (Dąbrowska *et al.*, 2017; Kotla *et al.*, 2017; Ita, 2014). The transcellular pathway is a very selective route, involving the passage through both the corneocytes of the epidermis. Hydrophilic substances will prefer this route, although they have still to partition between the corneocytes and the lipid matrix, to jump from one corneocyte to another one (Dąbrowska *et al.*, 2017; Moser *et al.*, 2001). The transappendageal route involves appendages (sweat glands, hair follicles) and is a typical route for the penetration of large and ionic substances. Covering approximately 0.1 % of the skin surface the contribution of the transappendageal route is considered the least significant passage of penetration, but may be of importance for the penetration of some substances, such as nanoparticles (Dąbrowska *et al.*, 2017; Lane, 2013).

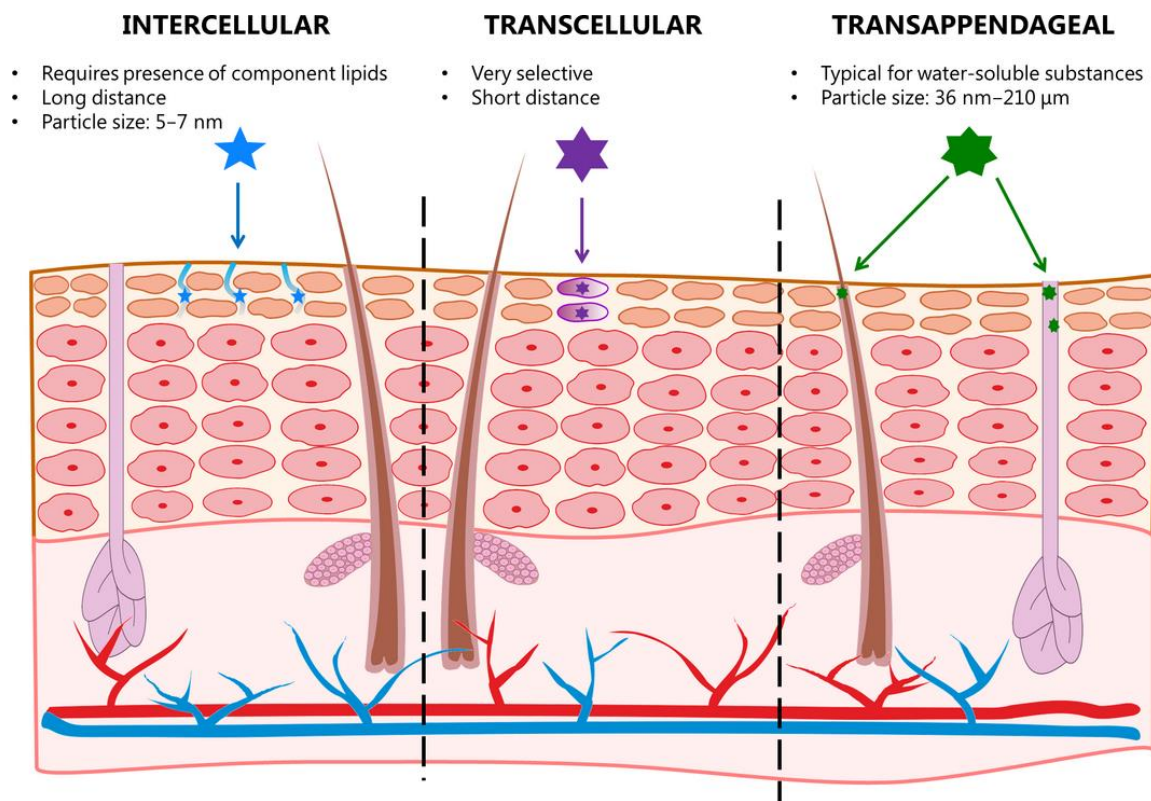


**Figure 2:** Penetration pathways through the stratum corneum barrier (Dąbrowska *et al.*, 2017) (Copyright© reprinted with permission from RightsLink®).

## 1.2 Wounds

An acute wound occurs when the barrier function of the skin is compromised by injury such as torn, cut or puncture, which consequently could result in serious morbidity and mortality (Hussain *et al.*, 2017; Deb *et al.*, 2018). The human body responds to this injury by initiating the wound-healing process thus restoring the skin barrier function, tissue integrity and homeostasis. Several factors can affect and impair the healing process and complicate the wound restoration, causing the wound to be chronic (Hussain *et al.*, 2017).

### 1.2.1 Wound healing process

The physiological process of wound healing involves several overlapping phases, namely hemostasis, the inflammatory phase, the proliferation phase, and the maturation phase. Hemostasis is a rapid process stopping and controlling the bleeding immediately upon injury, and serves as a foundation in the wound healing process. The inflammation process involves accumulation of inflammatory mediators leading to dilation of blood vessels and increased

vascular permeability, where re-epithelialization, formation of blood vessels and formation of a provisional matrix are characterizing the proliferation phase. In the maturation phase, the wound healing ends with tissue remodeling and formation of scar tissue (Hussain *et al.*, 2017; Janis and Attinger, 2006). **Figure 3** summarizes the phases of wound healing and which cells are involved in each phase. If disruption of the wound healing phases or unsuccessful restoration of structural integrity occur, the wound is considered to have entered the chronic state (Stadelmann *et al.*, 1998).

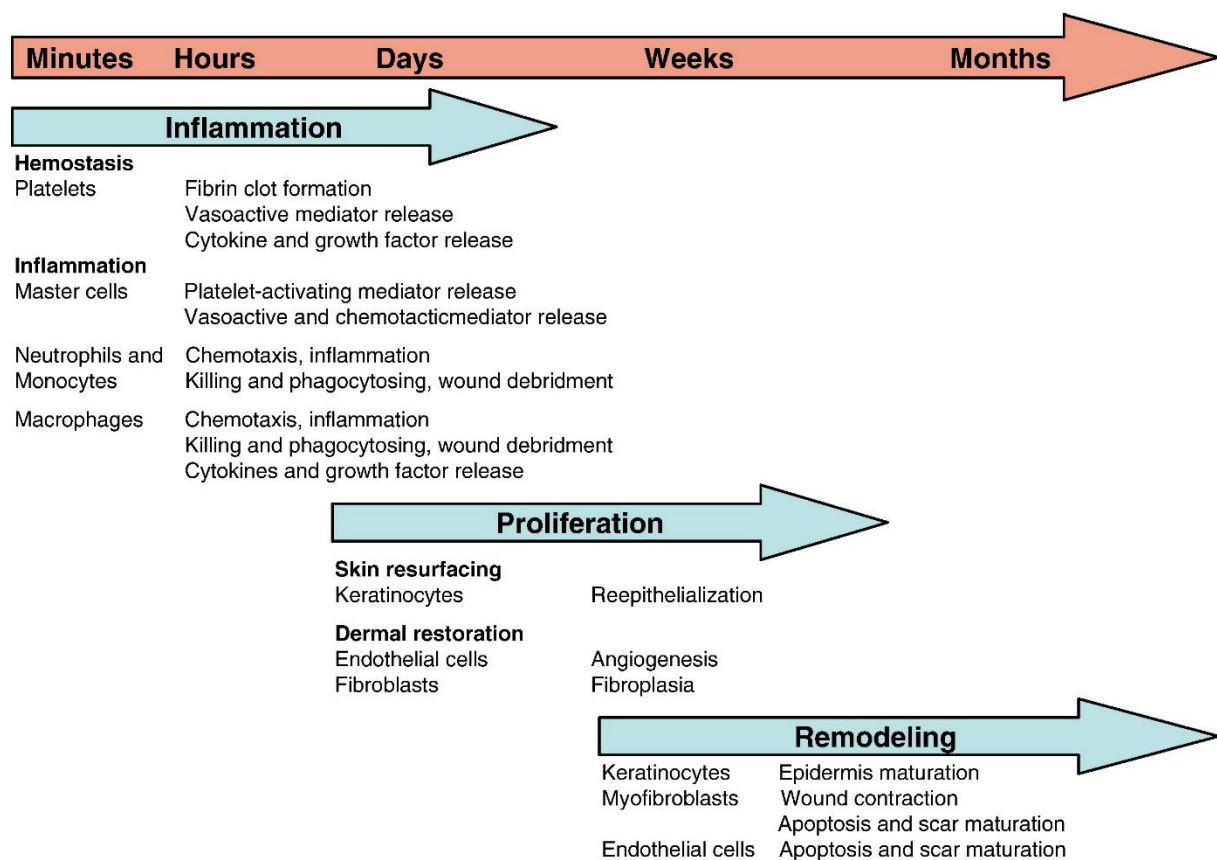


**Figure 3:** Wound healing phases including the involved cells (Li *et al.*, 2007) (Copyright© reprinted with permission from RightsLink®).

### 1.2.2 Chronic wounds

Chronic wounds include diabetic ulcers, vascular ulcers and pressure ulcers and represent a major challenge in global healthcare due to the difficulty in treatment and high healthcare costs (Ashtikar and Wacker, 2018). While acute wounds heal according to the phases described in section 1.2.1, chronic wounds have a disruption in the wound healing phases, often caused by

persistent inflammatory phase (Morton and Phillips, 2016; Frykberg and Banks, 2015). Chronic wounds are, in many cases, a result of secondary complication to other comorbid diseases or modulating factors, like diabetes, obesity, malnutrition, smoking or stress which could complicate the treatment (Wernick and Stawicki, 2018; Hussain *et al.*, 2017). In addition, as the wound fails to heal, the exposure to bacteria from the surrounding skin and environment often leads to colonization of bacteria and infection in the wounded area, resulting in increased morbidity and mortality (Simões *et al.*, 2018).

### **1.2.3 Conventional treatment of chronic wounds**

Conventional treatment of chronic wounds is based on wound dressings to protect the wound from decontamination from the outside environment. The majority of the conventional wound dressings like gauze, cotton wool and bandages have some drawbacks. They can give bacterial protection to some extent, but moist from the exudate or outside could easily compromise this barrier. In addition, little occlusion keeps the wound environment from being optimal by evaporation of moisture, and adhesion of the dressing to the wound makes them painful to remove (Boateng and Catanzano, 2015). Since the conventional dressings do not have an active role in the process of wound healing, they are to a greater extent being replaced by more advanced dressings. These more advanced dressings can exert an intrinsic biological activity due to their material composition or can incorporate drugs taking part in the healing process. The individual differences in patients with chronic wounds and the many phases of the wound healing process make the treatment challenging and complicated. The fact that one cannot generalize that one dressing is suitable for the treatments of all chronic wounds, addresses the need of further development of advanced dressings with a multi-targeted approach (Boateng and Catanzano, 2015).

### 1.3 Curcumin

Curcumin (1,7-bis[4-hydroxy-3-methoxyphenyl]-1,6-heptadiene-3,5-dione) is a natural polyphenol found in the rhizome of *Curcuma longa* (turmeric plant) (**Figure 4**)



**Figure 4:** *Curcuma longa* with its rhizome and powder

<http://ottawavalleydogwhisperer.blogspot.no/2012/11/turmeric-and-curcumin-good-for-your.html>

*Curcuma longa* is a plant in the *Zingiberaceae* family and has had a central role in Indian Ayurvedic medicine for many years due to its abundant health benefits. The curcumin powder originates from the dried rhizome of the *Curcuma longa*, and is composed of several structurally related curcuminoids, namely diferuloylmethane/curcumin (75 %), demethoxycurcumin/curcumin II (20%) and bisdemethoxycurcumin/curcumin III (5%) (Mohanty and Sahoo, 2017). The chemical structures of the curcuminoids are presented in **Figure 5**.

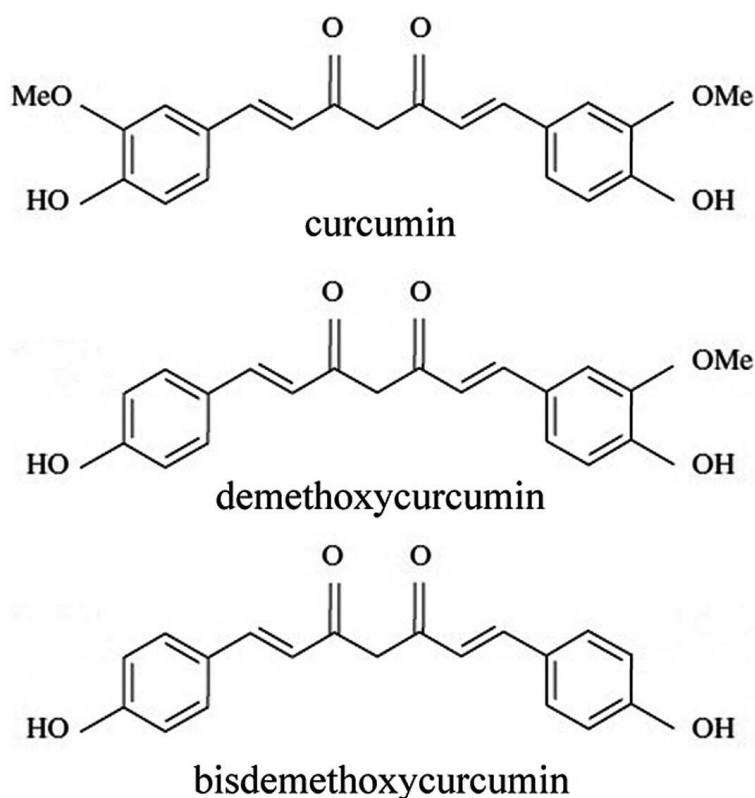


**Figure 5:** Chemical structure of the different curcuminoids (<https://www.spandidos-publications.com/10.3892/mmr.2012.1106> )

Curcumin has gained attention as a potential therapeutic agent due to its remarkable applicability in the treatment of numerous diseases. Several studies have been exploring its therapeutic potential for a wide range of chronic diseases such as cardiovascular diseases, neurodegenerative disorders like Alzheimer disease, Parkinson’s disease and multiple sclerosis, autoimmune diseases such as rheumatoid arthritis, pulmonary diseases, metabolic disease and diabetes mellitus type II and psychological diseases. Among the abundant health benefits, curcumin and its derivatives are also known for promoting healing of cutaneous, acute and chronic wounds (Mehanny *et al.*, 2016; Hussain *et al.*, 2017).

### 1.3.1 Curcumin in wound healing

Curcumin is one of the most studied phytochemical regarding wound healing, and its potential as a wound healing agent is attributed to its anti-inflammatory, anti-infectious and anti-oxidant activities (Mehanny *et al.*, 2016). Curcumin is suggested to be able to influence several phases in the wound healing process, such as the inflammatory phase, proliferation phase and the

remodeling phase. Its effects on the inflammatory phase are due to its ability to act as a free-radical scavenger thereby reducing oxidative stress and tissue damage (Akbik *et al.*, 2014). Advanced re-epithelialization, enhanced formation of new blood vessels and higher granulation tissue formation are suggested effects on the proliferation phase, while improving wound contraction in the remodeling phase (Mohanty and Sahoo, 2017). Despite its health benefits, curcumin is a poorly water soluble compound, with low oral bioavailability. Moreover, it is a photo-sensitive molecule and is rapidly degraded. Upon oral administration curcumin goes through extensive first-pass metabolism and its topical administration might be a promising alternative to overcome these challenges (Akbik *et al.*, 2014). On the other hand, the hydrophobicity of curcumin makes the formulation of wound dressing challenging, and challenging for topical administration at the wound site. Polyphenol compounds are also known to produce a toxic response in high doses upon topical administration (Mohanty and Sahoo, 2017).

## **1.4 (Trans)dermal delivery**

Transdermal administration involves administration of substances through the skin for systemical treatment, while dermal administration involves local treatment for dermatological conditions. Avoiding hepatic first-pass metabolism and gastro-intestinal side effects, (trans)dermal delivery can yield several advantages over other routes of administration. However, the barrier property of the *stratum corneum* limits drug penetration through/into the skin, and different strategies to overcome this limitation have been established (Foldvari and Kumar, 2017).

### **1.4.1 Improvement of dermal delivery**

Different techniques have been established to overcome the *stratum corneum* barrier thus enhancing drug penetration through the skin. These include the use of penetration enhancers, drug delivery systems, supersaturated solutions and physical methods. Chemical methods are based on the application of penetration enhancers to improve the penetration over the *stratum corneum*. By partitioning into and interacting with the skin barrier, penetration enhancers (surfactants, fatty acids, terpenes and solvents) promote a limited and reversible increase in permeability. A major drawback is their capability of inducing irritation in the skin (Dragicevic

and Maibach, 2017). Among the physical methods, i) microneedles technology involves creation of larger transport routes in the skin using microscopic needles, ii) sonophoresis employs low-frequency ultrasound enabling penetration pathways through the corneocytes, iii) electroporation with application of high-voltage pulse forms aqueous pathways across the skin lipid bilayer, iv) magnetophoresis achieves flux-enhancement by applying magnetic fields and inducing mechanical forces to drive charged particles into the skin (Dragicevic and Maibach, 2017; Foldvari and Kumar, 2017). Nanotechnology and the use of nanoparticulate systems to improve dermal drug delivery have also appeared to be promising as carrier systems to enhance drug penetration through the skin (DeLouise, 2012).

## **1.5 Nanotechnology**

A lot of devotion have been invested the later years in nanotechnology due to its potential to revolutionize the management of disease in terms of diagnostics, treatment and prevention (Prow *et al.*, 2011). Drug delivery based on nanotechnology has been of great importance in pharmaceutical research, aiming for the production of new and innovative formulations as well as improvement of already existing delivery systems. Including a broad range of carrier systems, nanoscale drug delivery is developed with the ambition to overcome the limitations related to dermal drug delivery, such as poor solubility, bioavailability, limited stability and penetration through the *stratum corneum* (Banerjee, 2013). The most well-established nanoscale carrier system is today represented by the liposomes (Riehemann *et al.*, 2009) further described in section 1.5.1.

### **1.5.1 Conventional liposomes**

Since their discovery, liposomes as a drug delivery systems have been a field of great interest and study. Liposomes are lipid-based nanovesicles consisting of single or multiple lipid bilayers encapsulating a hydrophilic core (**Figure 6** and **Figure 8 A**).

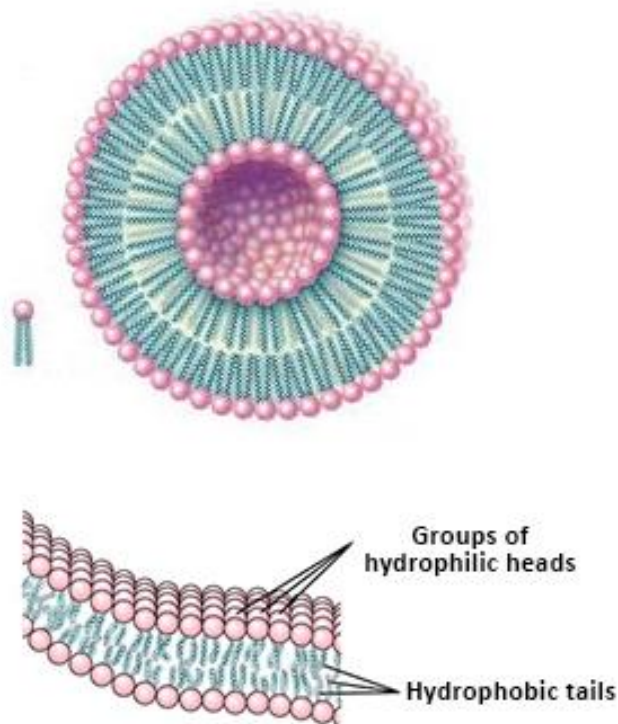


**Figure 6:** Composition of liposome and its lipid bilayer (<http://fortiferrum.com/liposomal-microencapsulated-iron?lang=en>)

The peculiar structure enables liposomes to incorporate both hydrophilic, lipophilic and amphiphilic drugs. The hydrophilic drugs will be located in the aqueous core, the lipophilic in the lipid bilayer and the amphiphilic divided in the two compartments (Bozzuto and Molinari, 2015). The main constituent of liposomes are natural or synthetic phospholipids. The type and amount of phospholipids used in the preparation, as well as the ionic and charge properties of these, are important factors determining the final structure of liposomes (Sala *et al.*, 2018). (Sala *et al.*, 2018). In addition, the preparation method affects the size and lamellarity of the liposomes. The liposomal structures are classified by their size and number of bilayers (De Leeuw *et al.*, 2009). The different classifications are illustrated in **Figure 7**.

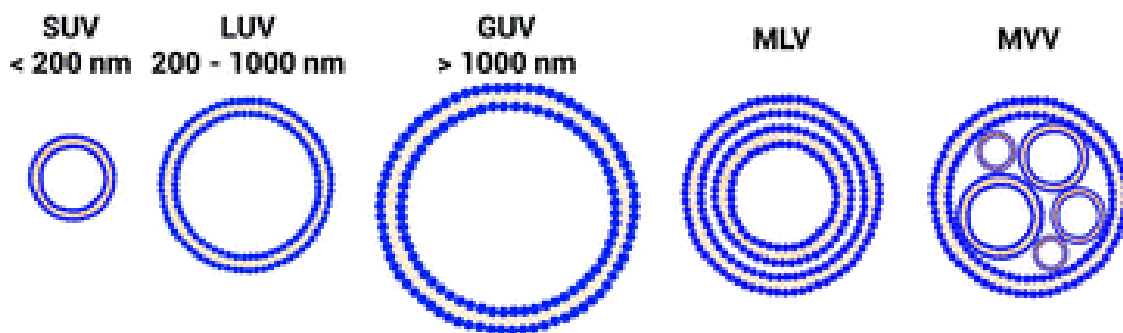


**Figure 7:** Classification of liposomes after size and number of bilayers. LUV – Large uni-lamellar vesicles, SUV – Small uni-lamellar vesicles, MLV – Multi-lamellar vesicles, GUV – Giant uni-lamellar vesicles (Grimaldi *et al.*, 2016) (Copyright© reprinted with permission from RightsLink®).

### 1.5.2 Deformable liposomes

Deformable liposomes are elastic lipid vesicles consisting of phospholipids and surfactants incorporated into the lipid bilayers (illustrated in **Figure 8 B**) (Siler-Marinkovic, 2016). The incorporation of surfactant leads to the softening of the bilayer membranes, thus increasing their flexibility. This increased flexibility compared to the conventional liposomes, allows them to squeeze through the *stratum corneum* and deliver the drug in the deeper skin layers (Elsayed *et al.*, 2006). Their passage through skin is driven by the osmotic gradient across the epidermis (Cevc and Blume, 1992). Deformable liposomes can also act as a depot and assure controlled and sustained release of the incorporated drug (Mota *et al.*, 2017).

### 1.5.3 Other liposomes

Ethosomes are flexible lipid vesicles and are mainly composed of phospholipids as conventional and deformable liposomes. In addition, the ethosomes have a relative high alcohol content (20-40 %), increasing the lipid bilayer fluidity (Rakesh and Anoop, 2012). The ethosomal structure is illustrated in **Figure 8 D**. Ethosomes are mainly used for trans(dermal) delivery because of their enhancement of drug penetration into the deeper layers of the skin compared to the conventional liposomes (Ainbinder *et al.*, 2016; Satyam *et al.*, 2015). The mechanism of enhanced skin penetration is considered to be in conjunction with the fluidizing effect of ethanol on the bilayer as well as rearrangement of skin lipids in the *stratum corneum* (Ainbinder *et al.*, 2016).

Another type of flexible lipid carrier proposed to enhance skin penetration of drugs is the PG deformable liposomes. These are composed of phospholipids, PG and water, and are promising nanocarriers for topical delivery. Embedded in the lipid bilayer, PG has been expected to increase the incorporation of drug and the stability of the formulation (Elsayed *et al.*, 2007a).

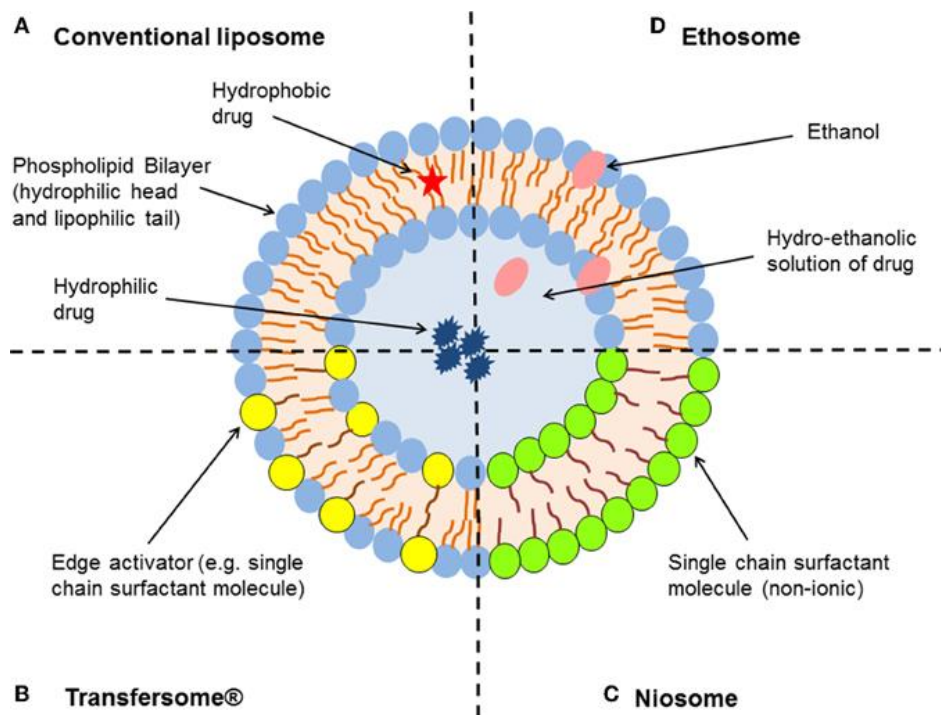


**Figure 8:** Schematic overview of some of the different types of liposomes and their composition (Hua, 2015) (Copyright© reprinted with permission from RightsLink®).

#### 1.5.4 Liposomes in wound dressings

Nanoformulations such as liposomes containing a variety of drugs could be incorporated into medical dressings used in the treatment of chronic wounds to modulate the phases of wound healing. The incorporated drugs could act as cleansing agents, debriding agents or anti-microbial agents aiding the healing process. Liposomes could, in addition, provide sustained release of the incorporated drug, thereby reducing the need for frequent change of wound dressings and associated pain for the patient. Still, more research needs to be done using formulations based on nanotechnology for wound healing (Ashtikar and Wacker, 2018; Boateng and Catanzano, 2015).

## 2 Aim of the study

The main aim of this study was to develop and optimize effective lipid-based nanosystems for dermal delivery of curcumin.

The aim was divided in the following:

- Development of deformable liposomes of different surface charge (cationic, anionic and neutral) containing curcumin, and their characterization in respect of size, zeta potential, entrapment efficiency and stability
- Determining the penetration potential of liposomal curcumin through *in vitro* curcumin release and *ex vivo* curcumin penetration through full thickness human skin, focusing on the effect of liposomal surface charge
- Evaluation of the anti-inflammatory activity of the deformable liposomes
- Evaluation of the anti-bacterial activity of liposomal curcumin against *S. aureus* and *S. pyogenes*
- Proving the safety of the novel liposomal formulations through *in vitro* cell toxicity study
- Evaluation of the cell proliferative effect of deformable liposomes in human skin fibroblasts.



## 3 Materials and methods

### 3.1 Materials

#### 3.1.1 Materials used

Albunorm<sup>®</sup> 200 g/L, Octapharma AS, Jessheim, Norway

Ammonium molybdate, Sigma-Aldrich, Chemie GmbH, Germany

Cell Counting Kit-8 (CCK-8), Sigma-Aldrich, Chemie GmbH, Germany

Curcumin, Sigma-Aldrich, Chemie GmbH, Germany

Dulbecco's modified Eagle's medium (DMEM), Sigma-Aldrich, Chemie GmbH, Germany

Ethanol, Sigma-Aldrich Chemie GmbH, Germany

Fetal bovine serum, Sigma-Aldrich Chemie GmbH, Germany

Fiske-SubbaRow reducer agent, Sigma-Aldrich Chemie GmbH, Germany

Griess reagent, Sigma-Aldrich Chemie GmbH, Germany

Sulfuric acid, May & Baker LTD (Dagenham, UK)

Chloridric acid, Sigma-Aldrich Chemie GmbH, Germany

Human foreskin fibroblasts (HFF), ATCC, Manassas, USA

Hydrogen peroxide 30%, Merck, Darmstadt, Germany

Lipoid S100, Lipoid GmbH, Ludwigshafen, Germany

Lipopolysaccharide (LPS; *Escherichia coli*, 055:B5), Sigma-Aldrich Chemie GmbH, Germany

Methanol, VWR International S.A.S., Fontenay-sous-Bois, France

Murine macrophage RAW 264.7 cells, ATCC, Manassas, USA

Octadecylamine, Sigma-Aldrich Chemie GmbH, Germany

Penicillin-Streptomycin, Sigma-Aldrich Chemie GmbH, Germany

Phosphorus standard solution, Sigma-Aldrich Chemie GmbH, Germany

Polysorbate 20, Sigma-Aldrich Chemie GmbH, Germany

Potassium phosphate monobasic, Sigma-Aldrich Chemie GmbH, Germany

Propylene glycol, Sigma-Aldrich Chemie GmbH, Germany

RPMI 1640 medium, Sigma-Aldrich Chemie GmbH, Germany

Sodium chloride, Sigma-Aldrich Chemie GmbH, Germany

Sodium deoxycholate, Sigma-Aldrich Chemie GmbH, Germany

Sodium phosphate dibasic dehydrate, Sigma-Aldrich Chemie GmbH, Germany

### **3.1.2 Equipment and devices**

Biofuge stratos centrifuge, Heraeus instruments, Germany

Branson 5510 Ultrasonic Cleaner, Marshall Scientific, Hampton, New Hampshire, USA

BÜCHI Rotavapor R-124, Büchi laborstechnik, Flawil, Switzerland

BÜCHI Vacuum Pump V-700, Büchi laborstechnik, Flawil, Switzerland

BÜCHI Waterbath B-480, Büchi laborstechnik, Flawil, Switzerland

Julabo Refrigerated/Heating Circulator F12-ED, Julabo GmbH, Seelbach, Germany

Multi-station Franz diffusion cell system, PermeGear Inc., Bethlehem, USA

NICOMP Submicron particle sizer, model 370, Nicomp Particle sizing systems, Santa Barbara, California, USA

Nucleopore® Track-Etched Polycarbonate Membranes 0.8µm, 0.4µm, 0.2µm, Whatman International Ltd., Maidstone, UK

Sension+ PH31 pH-meter, Hach, Loveland, USA

Sonics High Intensity Ultrasonic Processor 500 Watt Model with Temperature Controller

Malvern Zetasizer Nano – ZS, Malvern, Oxford, UK

### **3.1.3 Software**

Photon correlation spectroscopy: CW388 Version 1.68 – NICOMP Particle Sizing Systems, Santa Barbara, California, USA

Zeta potential: Zeta potential report version 2.2, Malvern instruments Limited, Malvern, UK

## 3.2 Methods

### 3.2.1 Preparation of phosphate buffer saline (PBS)

PBS was prepared by dissolving disodium hydrogen phosphate (2.98 g/L), monobasic potassium phosphate (0.19 g/L) and sodium chloride (8.00 g/L) in Milli-Q water. When the powders were completely dissolved the pH were adjusted to 7.4.

### 3.2.2 Preparation of conventional liposomes

The conventional liposomes were prepared by the thin film hydration method according to Ternullo *et al.* (2017). The method is illustrated in **Figure 9**.

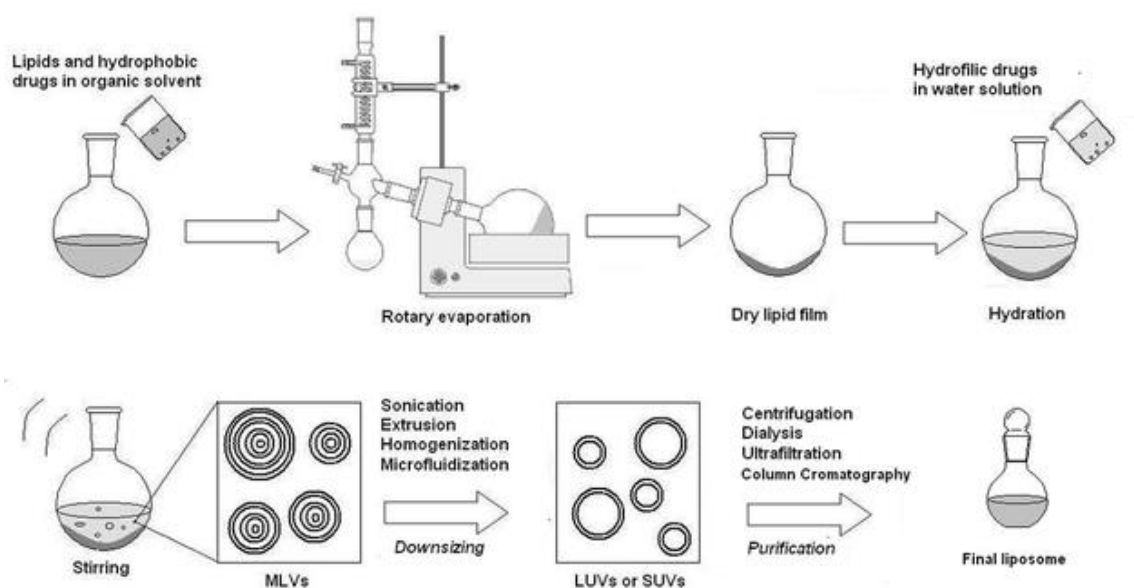


**Figure 9:** Schematic of conventional thin film hydration method (<http://www.intechopen.com/source/html/44386/media/image7.png>).

Phosphatidylcholine (200 mg) and curcumin (20 mg) were weighed in a round bottom flask and dissolved in methanol. The volume of methanol was adjusted to assure that both lipid and curcumin were fully dissolved. Methanol was removed through evaporation using a rotary evaporator. The rotary evaporator water bath was set to hold a temperature of 45 °C, the rotation to 70 rpm, and the pressure was regulated down to 55 mmHg. When the evaporation of the organic solvent was completed, the round bottom flask was left in the rotary evaporator water

bath for additional 1 hour under rotation (100 rpm) at 55 mmHg to ensure that no traces of organic solvent were present. The obtained dry lipid film was re-suspended in 10 ml of PBS and manually stirred until completely dislodged. The liposome suspension was stored in the fridge (4 °C) for 24 hours prior characterization and further handling.

### 3.2.3 Deformable liposomes

The deformable liposomes were also prepared by the thin film hydration method as the conventional liposomes (Section 3.2.2) (Ternullo *et al.*, 2017). However, in addition to curcumin and phosphatidylcholine, different surfactants were added to prepare cationic, anionic and neutral deformable liposomes. Octadecylamine and polysorbate 20 were included for cationic deformable liposomes, sodium deoxycholate for anionic, and polysorbate 20 for neutral. **Table 1** provides a complete overview of the composition of the deformable liposomes.

**Table 1:** Composition of the curcumin-loaded deformable liposomes.

<b>Deformable Liposomes</b>	<b>Curcumin (mg)</b>	<b>Phosphatidylcholine (mg)</b>	<b>Sodium deoxycholate (mg)</b>	<b>Octadecylamine (mg)</b>	<b>Polysorbate 20 (mg)</b>
<b>Cationic</b>	20	153	-	17	30
<b>Anionic</b>	20	170	30	-	-
<b>Neutral</b>	20	170	-	-	30

### 3.2.4 Ethosomes

Ethosomes were prepared using the ethanol-injection method developed by Thapa and co-workers, with some modifications (Thapa *et al.*, 2013). Briefly, 200 mg of phosphatidylcholine and 20 mg of curcumin were dissolved in 4 ml of concentrated ethanol. Under the constant stirring with a magnetic stirrer (600 rpm), 6 ml of PBS were slowly injected through a 21 G needle (0.8 x 40 mm). The suspension was left under stirring for 30 minutes.

### 3.2.5 Propylene glycol (PG) deformable liposomes

PG deformable liposomes were prepared by the modified ethanol injection method (Vanić *et al.*, 2014). Curcumin (20 mg) was dissolved in a mixture of PG (1 g) and 4 ml of PBS. Phosphatidylcholine (200 mg) was dissolved in 1 ml of ethanol and rapidly injected into the PG buffer solution under constant stirring (600 rpm) and the stirring continued for 30 minutes. The final liposome suspension was diluted with PBS to obtain a volume of 10 ml.

## 3.3 Size reduction

The size of all liposomes was reduced by applying the extrusion or sonication. For the extrusion, the polycarbonate membranes of the pore sizes of 800, 400 and 200 nm, respectively were used. For the sonication, a high intensity ultrasonic processor with temperature controller was employed.

### 3.3.1 Extrusion

Using a 10-ml syringe, the liposomal suspensions were forced through polycarbonate membrane filters with defined pore sizes to obtain a final liposome size between 200-300 nm. The first extrusion was through an 800 nm pore size membrane. The process was repeated through 400 and 200  $\mu\text{m}$  pore size membranes until desirable vesicle size of 200-300 nm were obtained. **Table 2** summarizes the exact extrusion procedures including the different membrane filters.

**Table 2:** Cycles of extrusion for the different types of deformable liposomes containing curcumin.

<b>Liposomes</b>	<b>Cycles of extrusion</b>
<b>Cationic deformable liposomes</b>	5 x 800 nm, 2 x 400 nm
<b>Anionic deformable liposomes</b>	5 x 800 nm, 7 x 400 nm
<b>Neutral deformable liposomes</b>	5 x 800 nm, 4 x 400 nm

### **3.3.2 Sonication**

The liposomal suspension was transferred to a glass vial and placed on ice. The suspension was exposed to ultrasonic irradiation. The sonication time was adjusted to obtain the desired particle size (200-300 nm), and lasted for 35 seconds for the conventional liposomes. The deformable liposomes were not sonicated due to their high deformability. The output used for the sonication probe was 40 Watt, amplitude was set at 40 and probe temperature was controlled not to exceed 40 °C.

### **3.4 Size measurements**

The size of the liposomes was measured using photon correlation spectroscopy (dynamic light scattering). The determination of the size distribution was performed using the NICOMP submicron Particle Sizer model 370. Sample preparation was carried out in a laminar airflow bench to avoid any contamination of the samples. Sample tubes were filled with distilled water and sonicated for 15 minutes in ultrasonic bath before further rinsing with filtered PBS (0.22 µm membrane filter). The liposomal suspension was diluted using the filtered (0.22 µm membrane filter) PBS until an intensity ranging between 250 and 350 kHz was achieved. The measurements were performed at room temperature (23-24 °C). The vesicle mode and the intensity-weighted distribution were used throughout the measurements. For each sample, three replicates were performed with a run time of 10 minutes.

### **3.5 Zeta potential measurements**

The zeta potential was determined using a Zetasizer Nano Z 2600, Malvern Instruments. For the measurements, a folded capillary cell (DTS1070) was used. Before starting, the cell was rinsed with 5 ml of ethanol and 5 ml of filtered tap water (0.22 µm membrane filter) using a syringe. The samples were diluted 1:10 (v/v) with filtered water to obtain an attenuator between 5 and 8. Each measurement was performed at 25 °C with an equilibration time of 180 seconds. Three replicates were performed for each formulation.

### **3.6 Curcumin entrapment**

The liposomal suspensions were centrifuged in a Biofuge Stratos, Heareus Instruments to separate liposomes from the free (unentrapped) curcumin. The suspensions were centrifuged at 4000 rpm for 10 minutes. The supernatant was separated from the pellets, which were further re-suspended with 1 ml of PBS. The supernatant (curcumin-containing liposomes) was diluted in methanol to dissolve the lipids. The curcumin content was then determined by UV-Vis spectroscopy at 425 nm as wavelength (section 3.7). The entrapment was expressed as curcumin/lipid ratio (mg/mg). Lipids were quantified by the phosphorous assay (section 3.8).

### **3.7 Quantification of curcumin**

Curcumin was quantified by UV-Vis spectroscopy. Standard curve of curcumin in methanol and PBS (1:1, v/v) was used for the quantification of curcumin, and was prepared using a stock solution of curcumin in methanol, followed by the dilutions to obtain the concentration range of 1-20 µg/ml. Three replicates of each standard solution were prepared. Aliquot of each solution (200 µl) was pipetted into a 96-wells plate and the absorbance read at 425 nm. The absorbance was plotted against the concentration of the standard solutions to obtain the standard curve.

### **3.8 Phospholipid quantification**

For the quantification of phospholipids in the liposomes the Bartlett assay (Bartlett, 1959) based on calorimetric determination of inorganic phosphate was used. Fiske-SubbaRow reagent,

Ammonium molybdate (0.22%, w/v), and H<sub>2</sub>SO<sub>4</sub> (10N) were prepared as reagents to be used in the assay. The standard curve of phosphorus was made using phosphorus standard solution at the following concentrations: 1, 2, 3, 4, 6 and 8 µg/ml ( $r^2 = 0.979$ ). Three replicates of each solution (standard phosphatidylcholine solution, buffer solution and liposomes) were prepared by dilution in distilled water (1:100, v/v), and 1 ml of each sample and phosphorus standard solutions was added to conical test tubes. Sulfuric acid (0.5 ml) was added to the samples before incubating at 150-160 °C for 3 hours, with marbles covering the tubes to avoid evaporation. After incubation, the samples were cooled down and two drops of H<sub>2</sub>O<sub>2</sub> were added before incubating at 150-160 °C for additional 1.5 hours. The samples were again cooled down and 4.6 ml of 0.22% ammonium molybdate and 0.2 ml of Fiske-subbarow reagent were added and mixed properly using a vortex. The samples were then incubated for 7 minutes at 100 °C. The samples were cooled down and, if necessary, diluted, before 200 µl of each sample was pipetted into a 96 well-plate. The absorbance was then read at 830 nm.

### **3.9 *In vitro* curcumin release**

The *in vitro* release of curcumin from the different deformable liposomes was performed using a multi-stationed Franz diffusion cell system (**Figure 10**) (Ternullo *et al.*, 2017). The acceptor chambers used in the experiment were of a volume of 12.0 or 12.1 ml. Before the start of the experiment, the acceptor chambers were rinsed with distilled water before being filled with the receptor medium, which was a solution of PBS containing 5% (v/v) of Alburnorm<sup>®</sup>. The artificial membrane used for the *in vitro* skin penetration was cellophane. Cellophane was soaked in PBS 30 minutes before the experiment and then inserted between the donor and receptor chambers. The formulations to be tested, CDL, ADL and NDL, were prepared by diluting them at the same concentration (0.6 µg/ml). Aliquot (600 µl) of the prepared liposomal suspensions were added into the donor chamber at the start of the experiment. The donor chamber and sampling port were covered with triple layers of parafilm to avoid evaporation. The experiment was carried out for 24 hours at 32 °C. Samples (500 µl) were withdrawn at certain time intervals, namely every hour for 8 hours and at 24 hours. To maintain the sink conditions, the withdrawn sample was replaced with an equal volume of fresh receptor medium. The experiments were performed in triplicates.

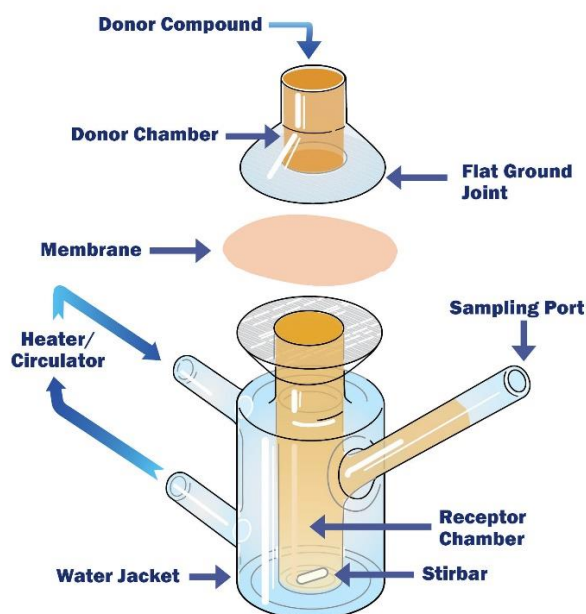


Figure 10: Schematic view of a Franz cell ([www.permeagear.com](http://www.permeagear.com))

To quantify the curcumin in the withdrawn samples from the receptor chamber, a standard curve of curcumin in PBS/Albunorm<sup>®</sup> solution was used. For this purpose, a stock solution of curcumin in ethanol was diluted with PBS buffer containing 5% Albunorm<sup>®</sup>. The concentration range was 0.25-20  $\mu\text{g/ml}$ . Three replicates of each solution were prepared. Each solution (200  $\mu\text{l}$ ) was pipetted into a 96-wells UV-plate and the absorbance measured at 425 nm.

### 3.10 *Ex vivo* skin penetration of curcumin

The *ex vivo* skin penetration experiments were carried out using the full thickness human skin in the same Franz diffusion cell system used for the *in vitro* curcumin release study. Human skin was obtained from the resected skin during abdominoplasty of female patients, after their written consent was received. No ethical approval was required by the Norwegian Ethical Committee, since the excess of skin panni is normally disposed after the surgery. The experiments were performed in accordance with the Declaration of Helsinki Principles. The obtained skin panni was cleared of the subcutaneous fat, washed with PBS and frozen at -20  $^{\circ}\text{C}$ . Prior to the experiment, the human skin was thawed at room temperature until completely defrosted. The full thickness human skin used in the experiments had a thickness ranging between 1.10 and 1.30 mm. The experiments were carried applying the same approach as for

the *in vitro* release experiments (section 3.9). Briefly, the liposomal formulations (same as for *in vitro* release studies) were diluted to the same concentration (0.6 µg/ml), and 600 µl of the samples were added into the donor compartment at the start of the experiment. Triple layers of parafilm were covering the donor chamber and sampling port to avoid evaporation. The experiment was carried out for 24 hours at 32 °C. Samples (500 µl) were withdrawn at certain time intervals, namely every hour for 8 hours and at 24 hours. To maintain the sink conditions, the withdrawn sample was replaced with an equal volume of fresh receptor medium. The experiments were performed in triplicates. For the quantification of the samples withdrawn from the receptor chamber the standard curve described in the previous section (section 3.9) was utilized.

### **3.11 Anti-inflammatory potential of liposomal curcumin**

The anti-inflammatory activity was determined by measuring the nitric oxide (NO) inhibition. The method used for the experiment is described by Basnet and collaborators (Basnet *et al.*, 2012). In the experiment, the effects of different formulations on the production of NO in lipopolysaccharide (LPS)-induced murine macrophage RAW 264.7 cells were determined. In a 24-well plate, cells ( $5 \times 10^5$  cells/ml) were cultured with RPMI 1640 medium supplemented with 10% fetal bovine serum and glutamine. The cells were incubated at 37 °C for 24 hours in 5% CO<sub>2</sub> allowing them to stabilize and adhere. Aliquots (10 µl) of liposomal suspensions at various concentrations and 990 µl of LPS solution (1 mg/ml) were added to each well, and further incubated for 24 hours. After the incubation, the effect of the liposomal formulations on the production of NO was measured in terms of nitrite formation by mixing equal amounts of Griess reagent and the sample in the wells (350 µl sample + 350 µl Griess reagent). The measurements were performed in triplicates and absorbance was read at 540 nm. The samples to be tested for the anti-inflammatory activity were i) PG 20% (w/v) in PBS, ii) NDL, ADL and CDL, all of them with or without curcumin, respectively iii) free curcumin, namely curcumin in PG (20%) solution. Three different lipid concentrations were tested, namely 1, 5 and 10 µg/ml. The formulations not containing curcumin (negative controls) were diluted to have equal lipid concentrations as for liposomes containing curcumin. As a positive control, LPS (1 mg/ml) was used.

### **3.12 Anti-bacterial activity**

The *in vitro* anti-bacterial activity of curcumin-containing liposomes was tested using the broth micro-dilution method which involves a two-fold dilution of the samples (Balouiri *et al.*, 2016). Two clinical strains of bacteria tested in this experiment were *Staphylococcus aureus* MSSR476 and *Staphylococcus pyogenes* ATCC19615. For the preparation of bacterial suspension, colonies of bacteria were transferred aseptically into a sterile saline solution (0.85%) and vortexed. The density was then adjusted to 0.5 McFarland units, which corresponds to a bacterial suspension of  $1-2 \times 10^8$  CFU/ml. The so prepared bacterial suspension was further diluted in Mueller Hinton broth (1:150 as volume ratio, respectively). For *S. pyogenes*, Mueller Hinton agar with 5 % horse blood was used as growth medium. In a 96-well plate, 50  $\mu$ l of Mueller Hinton broth and 100  $\mu$ l of formulation to be tested were added. By transferring 50  $\mu$ l from the first to the 11<sup>th</sup> well a two-fold dilution was made. The 12<sup>th</sup> well was used as negative control and did not contain any formulation. Each well was inoculated with 50  $\mu$ l of microbial inoculum previously prepared as described above. The 96-well plate was incubated for 4 hours at 37 °C. An aliquot of sample (20  $\mu$ L) from each well was diluted 10 times in PBS and transferred to a Mueller Hinton broth plate and incubated overnight at 37 °C to allow growth of the survived bacteria. The bacteria colonies were counted and the bacterial survival (%) was determined. The counted colonies in negative control were referred as 100%. The formulations tested for anti-bacterial activity were empty deformable liposomes (cationic, anionic and neutral), deformable liposomes with curcumin (cationic, anionic and neutral), PG solution (20%) and curcumin in PG solution (20%). Curcumin concentrations in all tested formulations were 100 and 200  $\mu$ g/ml, respectively, while lipid concentrations were of 2 and 4 mg/ml, respectively.

### **3.13 *In vitro* cell toxicity and proliferation assay**

The method used for the *in vitro* cell toxicity and proliferation assay were based on the method of Gainza and co-workers (Gainza *et al.*, 2014). The cell line used for the assay was human foreskin fibroblasts (HFF). The cells were cultured on Dulbecco's modified Eagle's medium (DMEM) supplemented with 15% (v/v) fetal bovine serum and 1% (v/v) penicillin-streptomycin at 37 °C in 5% CO<sub>2</sub>. HFF were seeded in a 96-well plate at a density of 5000 cells/well. The plate was incubated for 24 hours at 37 °C and 5% CO<sub>2</sub>. Each formulation (10  $\mu$ l) was then added to the each well and the cells were cultured under the same conditions for

12 and 24 hours. To quantify the living cells after the treatment, 10  $\mu$ l of Cell Counting Kit-8 (CCK-8) were added in each well and incubated for further 4 hours. The absorbance was then read at 450 nm. The absorbance was directly proportional to the number of living cells in the culture. The formulations tested for the cell proliferation assay were i) PG solution 20%, ii) curcumin in PG solution 20%, iii) empty deformable liposomes (cationic, anionic and neutral), iv) curcumin-containing deformable liposomes (cationic, anionic and neutral). The concentration of lipids in the liposomal formulations were 1, 10 and 50  $\mu$ g/ml, respectively. Untreated cells were used as a negative control.

### **3.14 Stability of liposomes**

The stability of the liposomes containing curcumin was determined by measuring the vesicle size, zeta potential and entrapment efficiency after 1 month of storage at 4 °C.

### **3.15 Statistical analysis**

Statistical analysis was performed using one-way ANOVA test followed by Bonferroni's multiple comparisons test performed on GraphPad Prism version 7.00 for Windows (GraphPad Software, La Jolla CA, USA). A  $p$ -value < 0.05 was considered significant.

## 4 Results and discussion

The master project was focused on the development and optimization of liposomal formulations for improved dermal delivery of curcumin for treatment of chronic wounds. The effects of the liposomal surface charge on the skin penetration behaviour of deformable liposomes as well as the toxicity in HFF cells and anti-inflammatory response of curcumin-loaded deformable liposomes were examined. Moreover, as open wounds are highly exposed to bacterial infections, the anti-bacterial effect of curcumin-containing deformable liposomes was assessed.

### 4.1 Conventional liposomes

Conventional liposomes containing curcumin were prepared for comparison to deformable liposomes and were not the main focus of this project. The characteristics of conventional liposomes containing curcumin are summarized in **Table 3**.

**Table 3:** Characteristics of conventional liposomes containing curcumin ( $n=3 \pm SD$ ).

Liposome	Size (nm)	PI*	Zeta potential (mV)	Curcumin/lipid ratio (mg/mg)
Conventional liposomes	$260.23 \pm 3.62$	$0.18 \pm 0.02$	$-0.51 \pm 2.87$	$0.05 \pm 0.00$

\*Polydispersity index

The size was, as targeted, between 200-300 nm, and the polydispersity index (PI) rather low indicating good homogeneity of liposomal suspension. The zeta potential was found to correspond to the liposomal composition used in the preparation; PC liposomes are expected to be neutral and indeed our liposomes were displaying almost neutral zeta potential (-0.51 mV). To decide which of the size reduction method is more suitable for the application, both the extrusion and sonication method were applied and compared. Sonication leads to a more heterogeneous size distribution, where two populations of vesicle could be detected (**Table 4**), therefore extrusion was selected as better option.

**Table 4:** Size of empty conventional liposomes obtained through extrusion and sonication (n=3).

Size reduction method	Size (nm)
Extrusion	233.03 ± 8.51
Sonication	210.61 ± 2.94 (92.2%)
	335.56 ± 335.56 (7.8%)*

\*Two peaks representing two populations of liposomes

*In vitro* curcumin release studies of curcumin-loaded conventional liposomes were conducted using Franz diffusion cell system (section 3.9) using cellophane membrane and PBS containing 25 and 50 % PG as the receptor medium. Even with 50 % PG in the receptor medium, only a negligible amount of curcumin could be quantified after 24 hours (results not shown) indicating extremely low penetration. Modifications of the composition and structure of the conventional liposomes will result in lipid vesicles exhibiting enhanced penetration properties (Siler-Marinkovic, 2016), and we therefore decided to move towards deformable liposomes bearing different surface charge to enable better penetration of curcumin into the skin, as it would be beneficial for the wound therapy that curcumin can exhibit its anti-inflammatory, anti-bacterial and proliferative activities in the deeper skin/wound layers.

## 4.2 Deformable liposomes

Deformable liposomes are a good alternative to the conventional liposomes in enhancing skin delivery of different compounds enabling the delivery of the incorporated drugs in the deeper skin layers (Elsayed *et al.*, 2007b). The deformable liposomes were prepared by the thin film hydration method (section 3.2.3, **Table 1**) the incorporation of surfactants in the lipid bilayer of liposomes provides deformability of the lipid vesicles improving skin penetration of drugs. This is favored when hydrophobic non ionized drugs are incorporated in the vesicle (González-Rodríguez *et al.*, 2016). The effectiveness of drug delivery using deformable liposomes depends on several factors including the liposome size, surface charge and drug entrapment efficiency. The characteristics of deformable liposomes bearing different surface charge are summarized and presented in **Table 5**.

**Table 5:** Characteristics of the deformable liposomes containing curcumin. The results are expressed as mean  $\pm$  SD (n=3).

Deformable liposomes	Size (nm)	PI*	Zeta potential (mV)	Curcumin/lipid ratio (mg/mg)	Lipid recovery (%)
<b>Cationic</b>	231.5 $\pm$ 68.1 (90.4%)	0.2 $\pm$ 0.1	33.7 $\pm$ 1.1	0.04 $\pm$ 0.01	97.1
	392.3 $\pm$ 361.8 (9.6 %)				
<b>Anionic</b>	299.3 $\pm$ 22.8	0.2 $\pm$ 0.0	-34.9 $\pm$ 0.5	0.11 $\pm$ 0.01	89.1
<b>Neutral</b>	286.1 $\pm$ 60.8 (87.2%)	0.2 $\pm$ 0.0	-2.3 $\pm$ 0.3	0.07 $\pm$ 0.00	80.2
	130.8 $\pm$ 14.5 (12.8%)				

\*Polydispersity Index

#### 4.2.1 Size

The size obtained for the different deformable liposomes containing curcumin was between 200 and 300 nm, as targeted in this project. Although the polydispersity of liposomes was low (PI 0.2), there were still two populations of vesicles detectable, although in small percentages as compared to the main population. The size of the lipid vesicles influences the drug delivery to the skin (Baroli, 2010). The optimal size is proposed to be in the range between 200 and 300 nm thus providing the highest drug concentration in the reservoir offered by liposomes (du Plessis *et al.*, 1994). Extrusion technique through polycarbonate membrane was used to obtain the desired vesicle size allowing the production of lipid vesicles with a defined and well-characterized size distribution. The presence of surfactant in the phospholipid bilayers of the deformable liposomes provides them flexibility and elasticity, and extrusion will be a more gentle procedure as compared to sonication which would lead to destruction of liposomes and loss of incorporated curcumin. Moreover, the presence of surface-active components in the deformable liposomes could have a great effect on their size distribution, and it is suggested that a high concentration of surfactant covering the liposome surface could prevent aggregation upon extrusion (Bnyan *et al.*, 2018).

### **4.2.2 Polydispersity of deformable liposomes**

The polydispersity index (PI) is used to describe the distribution of vesicle size and takes into account the vesicle mean size, solvent refractive index, angle of measurement and variance in the distribution (Gaumet *et al.*, 2008). PI values above 0.3 are an indication of a wide size distribution, and lower values ( $< 0.1$ ) indicate a homogenous distribution of vesicle size. The PI for the deformable liposomes are presented in **Table 5** and were below 0.3 for all the lipid vesicles indicating a homogenous distribution for the deformable liposomes independently from the liposomal surface charge.

### **4.2.3 Surface charge**

The zeta potential corresponded to different surfactants used for the preparation of deformable liposomes. NDL exhibited a zeta potential near to neutral, while CDL and ADL showed positive and negative zeta potential, respectively, as expected (**Table 5**). The slightly negative surface charge of the NDL could be a result of negative charges on the phosphate group in the phosphatidylcholine molecules, however, it can be still considered as neutral. In addition to other physiochemical characteristics and their influence on dermal drug delivery, several authors have suggested that the modification of surface charge could have an impact on drug penetration into/through the skin as well (Ogiso *et al.*, 2001; González-Rodríguez *et al.*, 2016). In terms of stability, the surface charge might also play a central role, either through the creation of repulsive forces or agglomeration (Palac *et al.*, 2015). The stability could be improved by reduced aggregation caused by the electrostatic repulsion occurring between vesicles bearing similar charge on their surface.

### **4.2.4 Entrapment of curcumin**

Entrapment efficiency (EE) represents the fraction of the drug/active substance incorporated into the lipid vesicles in respect to total drug/active substance used in the preparation of the vesicles. To ensure improved skin deposition in respect of topical administration, a high incorporation of drug in the deformable liposomes is of great importance to assure sufficiently high drug concentration in the skin site thus exerting therapeutic effect. Several studies have been conducted to assess the effect of surfactant concentration on the EE of deformable liposomes, and it has been reported that lipid-surfactant ratios as well as surfactant type affect

the EE (Jain *et al.*, 2003; Bnyan *et al.*, 2018). El Zaaferany and co-workers proposed that the optimal lipid/surfactant ratio is 85:15% (El Zaaferany *et al.*, 2010), the same ratio used in our study for the preparation of deformable liposomes. The EE of curcumin in this study were found to be  $0.04 \pm 0.01$  mg curcumin/mg lipid for the CDL,  $0.11 \pm 0.01$  mg curcumin/mg lipid for the ADL and  $0.07 \pm 0.00$  mg curcumin/mg lipid for the NDL (**Table 5**). For all formulations, the highest entrapment was achieved for the ADL comprising sodium deoxycholate as surfactant. CDL showed the lowest EE with respect to the other formulations. Previous findings by Fang and collaborators indicated that octadecylamine as surfactant could induce repulsion with its positive charge in the phospholipid bilayer. This can cause changes in organization of the bilayer, thus affecting the accommodation of lipophilic drugs in the lipid bilayer (El Zaaferany *et al.*, 2010).

#### **4.2.5 Lipid content**

Although the extrusion is considered to be a rather gentle and efficient method to reduce the vesicle size, it can still result in a lipid loss due to precipitation of the lipid on the membranes. It is therefore crucial to determine the lipid recovery of lipid loss after the extrusion procedure is completed. Moreover, knowing the exact lipid concentration enables us to present the drug/lipid ratio (in our case curcumin/lipid ratio). The lipid recovery of the deformable liposomes is summarized in **Table 5**, and were greatest for the CDL (97.07%), whereas ADL and NDL had a lipid recovery of 89.07 % and 80.23% respectively. This indicates that cationic lipid composition is least affected by the extrusion process. The good lipid recovery (over 85 %) confirms that the quantified curcumin in liposomes is indeed curcumin associated with the phospholipid bilayers and not curcumin precipitation (Basnet *et al.*, 2012).

#### **4.3 *In vitro* curcumin release**

Skin penetration studies play an important role in the development of effective liposomal formulations for local administration and the choice of predictive models to assay *in vitro* penetration is highly important (Flaten *et al.*, 2015). For the *in vitro* release study, different formulations of deformable liposomes were investigated for their ability to deliver curcumin through a cellophane membrane for 24 hours using a Franz diffusion cell system (section 3.9). NDL showed the highest cumulative release of curcumin (2.6 %), whereas CDL showed very

limited release (0.5 %) and ADL showed no release through the artificial membrane. Curcumin is a lipophilic substance, and it is known that an increase in lipophilicity leads to a decrease in the skin permeability (Wenkers and Lippold, 1999). As for lipophilic drugs, a poor *in vivo/in vitro* correlation (IVIVC) could be observed, where *in vitro* testing tends to underestimate *in vivo* permeation of lipophilic compounds. It was suggested that the addition of solubilizing agents in the receptor medium could overcome this poor correlation (Agrawal *et al.*, 2015). In this study, we chose human serum albumin (HSA), which mimics the physiological conditions of the receptor medium to a higher extent and does not affect the membrane barrier function (Moser *et al.*, 2001). The ADL bear a negative surface charge similar to that of the cellophane membrane and the poor penetration could be due to repulsive forces acting between the surfaces of the same charge (Ternullo *et al.*, 2017). The neutral surface of NDL did not have any specific interactions with the cellophane membrane possibly explaining the highest curcumin release from those vesicles. The curcumin permeation profiles through cellophane are presented in **Figure 11**.

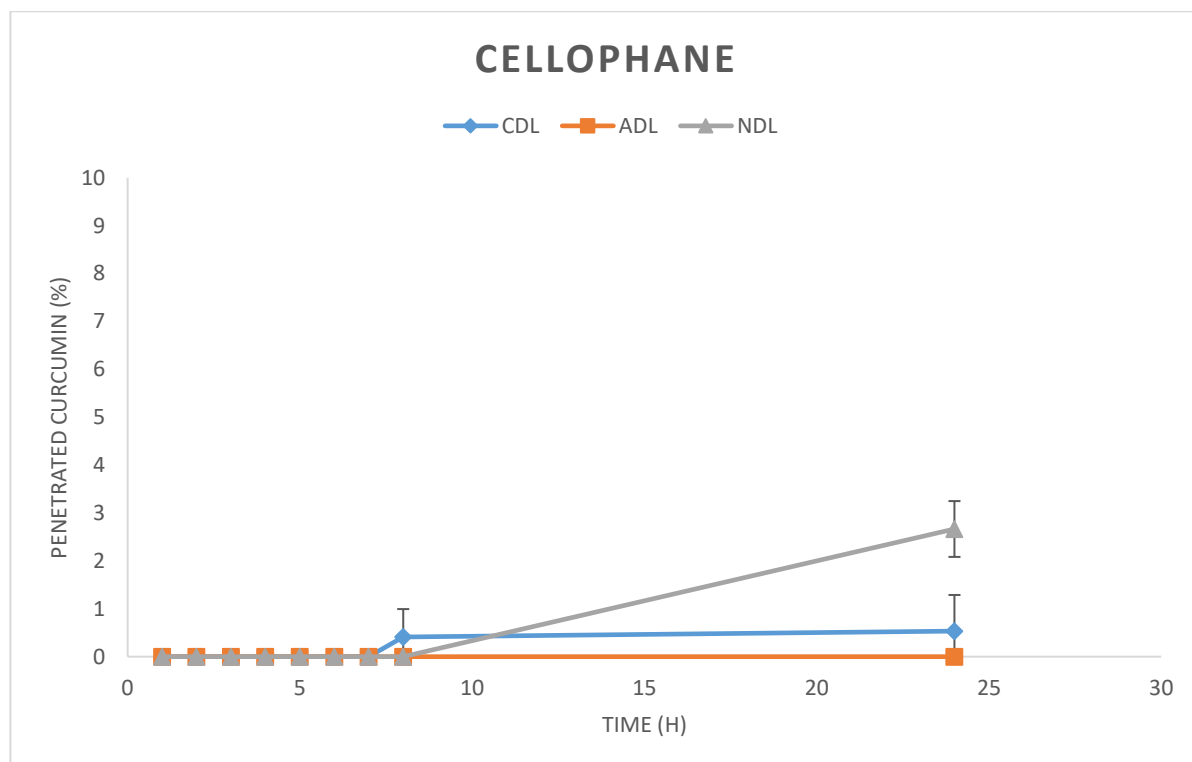


**Figure 11:** Penetration profile of curcumin from CDL, ADL and NDL through cellophane membrane. The results are presented as mean  $\pm$  SD (n=3)

Overall, the permeation of released curcumin was very low. However, cellophane membrane is rather poor model for testing skin penetration and served only for the obtaining preliminary data.

#### **4.4 *Ex vivo* skin penetration of curcumin**

The cumulative amount of penetrated curcumin through the full thickness human skin showed that ADL enabled the highest curcumin penetration (6.4 %), while CDL and NDL exhibited a slightly lower penetration (3.4 % and 4.2 %, respectively) (**Figure 12**). Although ADL exhibited the highest curcumin penetration, still very low amount of curcumin penetrated the full thickness human skin, in accordance with previous findings on curcumin-loaded lipid-core nanocapsules (Friedrich *et al.*, 2015). The full thickness human skin penetration profiles showed to be different compared to cellophane, emphasizing the importance of using an *in-vivo*-mimicking-membrane to assess the drug penetration through skin (Ternullo *et al.*, 2017). CDL exhibited a sustained penetration of curcumin compared to the other formulations, and this could be due to interactions with the *stratum corneum* cells. The corneocytes possess a negatively charged membrane. The interaction between this negative charge and the surface charge of the deformable liposomes could affect the diffusion through the skin, bearing in mind that similar charge leads to repulsion and opposite charge to attraction (Friedrich *et al.*, 2015). CDL could cause adsorption of negatively charged corneocytes in the *stratum corneum* leading to enhanced retention time and acting as a reservoir of drug within the skin layers. The reservoir would prolong the pharmacological action and reduce the frequency of administrations (González-Rodríguez *et al.*, 2016; Maestrelli *et al.*, 2010). This is especially relevant considering that our formulation was destined for wound therapy and that often application of wound dressings causes discomfort to the patients. Liposomal formulations with a negative surface charge have in previous studies shown to enhance the skin penetration of drug compared to both neutral and positively charged liposomes (Ascenso *et al.*, 2014; Gillet *et al.*, 2011). Cevc and Blume also stated that the presence of sodium deoxycholate lead to enhanced vesicle flexibility and allowed the liposomes to transport the entrapped drug into/through the deeper skin layers (Cevc and Blume, 2001).

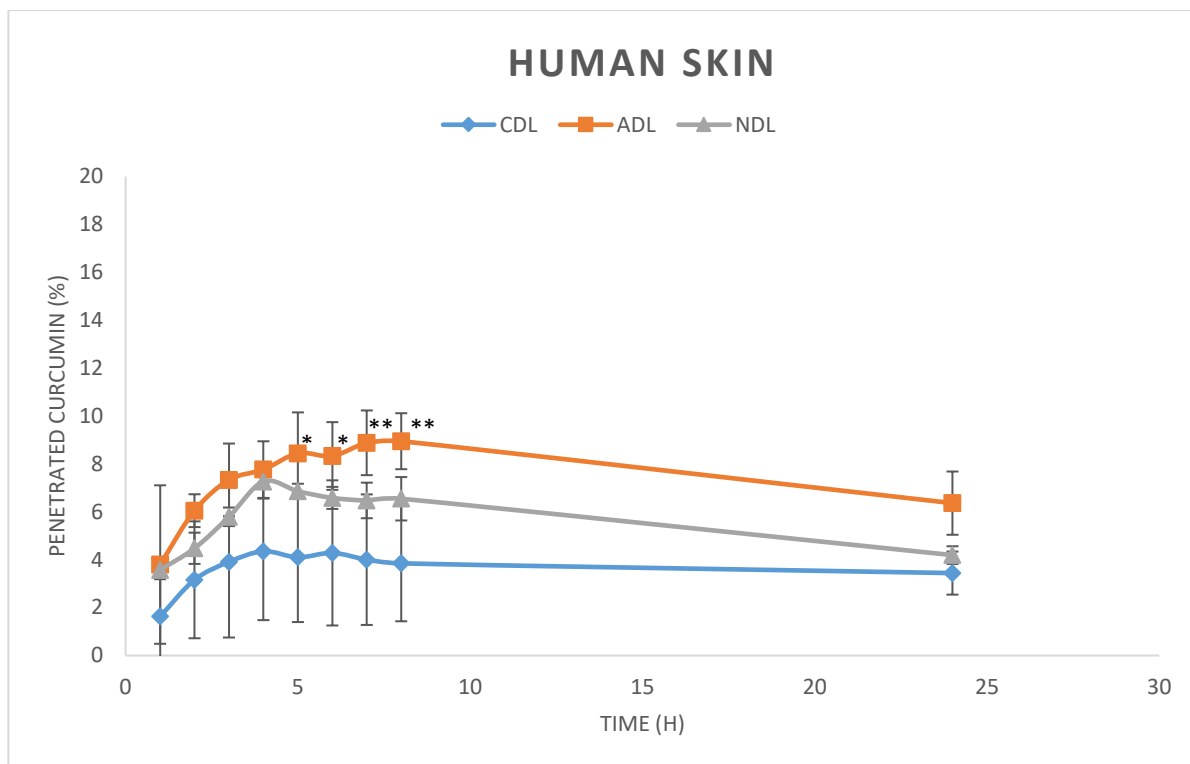


**Figure 12:** Penetration profile of curcumin from CDL, ADL and NDL through full-thickness human skin. The results are presented as mean  $\pm$  SD (n=3). \*Significantly higher (\*p < 0.05, \*\*p < 0.005) than CDL.

The amount of penetrated curcumin through the full thickness human skin from all formulations was higher compared to *in vitro* studies (cellophane membrane).

Since rather small amount of curcumin was able to penetrate the skin, we tried to determine where the remaining curcumin was located. Therefore, the amount of non-penetrated curcumin (retained on the top of the different skin membrane models) was quantified at the end of both *in vitro* and *ex vivo* experiments, and showed the difference between deformable liposomes. More CDL than ADL and NDL liposomes were found on the membrane/skin. This further confirms the previous findings and indicates the depot creation of CDL. **Figure 13** represents a summary of the curcumin penetration through both *in vitro* and *ex vivo* full thickness skin models. Due to the time limit, the amount of curcumin retained within the human skin was not quantified in this experiment, since it would require the development of an analytical method able to extract and determine curcumin in the presence of various proteins and other constituents of skin. However, we can postulate that a certain percentage of curcumin will be retained in the skin layers. This would probably indicate the accumulation of NDL in the skin is greater as compared to the CDL and ADL. However, one should consider that the penetration studies are mostly based on the intact skin and are not directly comparable with

damaged/wounded skin such as skin in chronic wounds. Our findings can therefore be used as an indication rather as a prove that same penetration pattern would be observed for skin with reduced barrier properties.

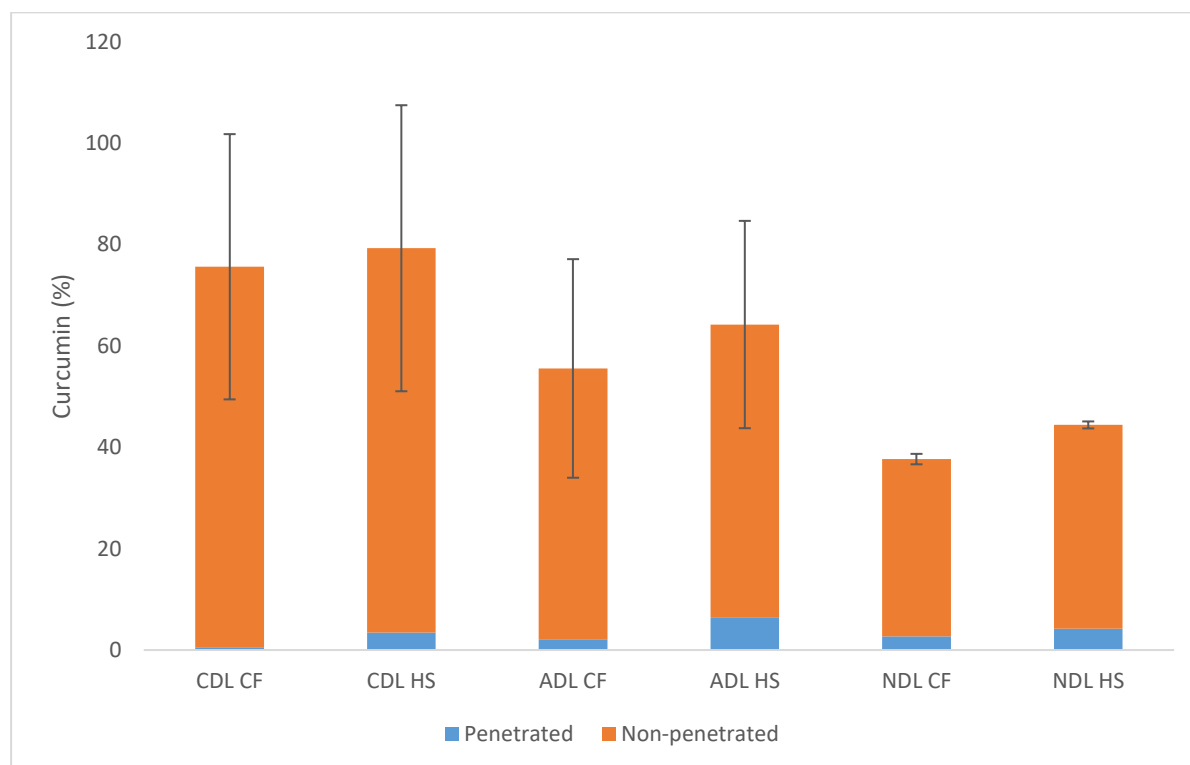


**Figure 13:** *In vitro* and *ex vivo* penetration (24 hours) of curcumin from deformable liposomes of different surface charge. The results are expressed as mean  $\pm$  SD ( $n=3$ ). (CF=Cellophane, HS=Human skin).

The findings also indicate that the type of the membrane used in the study influences the penetration profile to a certain degree (**Figure 13**).

#### 4.5 Ethosomes/PG deformable liposomes

Ethosomes were made containing ethanol (40 %, v/v) using a modification of the ethanol injection method (Thapa *et al.*, 2013) described in Section 3.2.4. Due to low incorporation of curcumin in the ethosomes, only one batch was prepared. The size of the ethosomes were in the targeted area, but a high PI was obtained, indicating a rather heterogeneous size population. The low EE did not assure a high drug concentration as wanted, therefore ethosomes were excluded from this project. The characteristics of the single batch made are summarized in **Table 6**.

**Table 6:** Characterization of ethosomes (n=1).

Size (nm)	PI	Zeta potential(mV)	Curcumin/lipid ratio (mg/mg)
<b>287.90 ± 93.92</b>	0.42 ± 0.02	-7.70 ± 0.44	0.02

The PG deformable liposomes were prepared using a modified ethanol injection method (Section 3.2.5.) Several batches were prepared, but problems with the extrusion (deposition of curcumin crystals in the polycarbonate membrane filter) and sonication applied as an alternative size reduction method, lead to the decision not to go further with this type of vesicles in this project. Both PG deformable liposomes and ethosomes are good candidates for topical delivery of drugs, and further optimization of preparation needs to be performed in a separate project.

#### **4.6 Anti-inflammatory potential of liposomal curcumin**

Inflammation is a normal part of the wound-healing process, and if prolonged, the wound may enter the chronic state and fail to heal. Contamination by pathogens, such as bacteria and viruses, initiates this inflammation, where nitric oxide (NO), alongside other radical species, plays an important role in mediating the inflammation process (Mohanty and Sahoo, 2017). For the anti-inflammatory testing the effect of curcumin-loaded deformable liposomes on the NO production in LPS-induced macrophages was assessed. LPS induces NO production. As a highly unstable radical NO will rapidly convert into  $\text{NO}_2^-$  or  $\text{NO}_3^-$  (Basnet *et al.*, 2012). All deformable liposomes showed an inhibitory effect on the NO production in LPS-induced macrophages. The results are presented in **Figure 14**. A dose dependent effect on the inhibition of NO production was observed for all tested formulations. Compared to curcumin in solution (free curcumin), the inhibitory effect on NO production was significantly higher when curcumin was incorporated into deformable liposomes. This enhanced effect of curcumin has been observed for other types of nanocarriers, such as conventional liposomes and nanospheres (Basnet *et al.*, 2012; Suwannateep *et al.*, 2012). The increased inhibitory activity of curcumin when formulated in deformable liposomes might be explained by an increased curcumin stability due to the liposomes' ability to protect curcumin against UV- and pH-induced degradation. Moreover, liposomes can enhance curcumin cellular uptake and improve curcumin

aqueous solubility thus maximizing its bioavailability and tissue distribution (Mehanny *et al.*, 2016; Suwannateep *et al.*, 2012). Among the different liposomes, the strongest effect was achieved when curcumin was incorporated in CDL. Similar findings have been obtained when curcumin was incorporated in PG liposomes (Zhao *et al.*, 2013). Curiously, the empty CDL showed the highest inhibitory activity as compared with the other formulations, suggesting the deformable liposomes exhibit anti-oxidant activity by themselves. This finding should be further explored as it might be providing a synergistic effect to CDL-associated anti-inflammatory agents. It would also be interesting to know whether the same activity of empty CDL would be maintained when CDL are incorporated in the secondary vehicle to serve as a wound dressing.

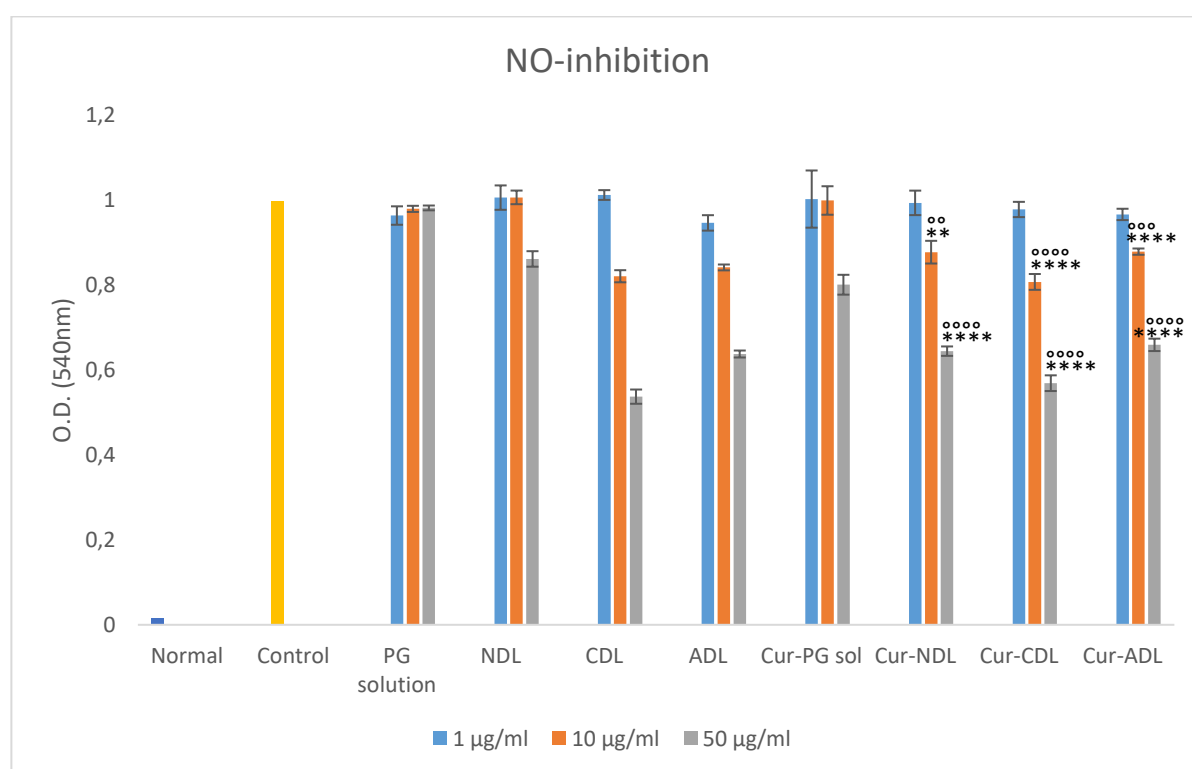


**Figure 14:** Effect of different formulations on nitric oxide (NO) production in lipopolysaccharide (LPS)-induced macrophages. The results are expressed as absorbance with mean  $\pm$  SD ( $n=3$ ). \*Significantly lower than control: \* $p < 0.03$ , \*\* $p < 0.002$ , \*\*\* $p < 0.0002$ , \*\*\*\* $p < 0.0001$ . °Significantly lower than CUR-PG: ° $p < 0.03$ , °° $p < 0.002$ , °°° $p < 0.0002$ , °°°° $p < 0.0001$ .

## 4.7 Anti-bacterial activity

Once skin is injured, microorganisms that normally are secluded to the surface of the skin gain entrance to the underlying tissues and could cause infection delaying the wound healing (Krausz *et al.*, 2015). The anti-bacterial activity of liposomal curcumin was tested against two Gram-positive bacteria (*S. aureus* and *S. pyogenes*), which are known to be predominant contaminants in chronic wounds (Simões *et al.*, 2018). The percentage of bacterial survival was calculated after comparing with negative control and is presented in **Table 7**. The different deformable liposomes and curcumin showed a great anti-bacterial potential against the two tested bacteria, namely *S. aureus* and *S. pyogenes*. CDL, both empty and containing curcumin, exhibited the strongest anti-bacterial effect. This effect could be explained by the ionic interaction and fusion with the bacterial cell envelope (Rukavina and Vanić, 2016). Cationic liposomes are on the other hand known to be more toxic than both neutral and anionic liposomes (Dokka *et al.*, 2000; Smistad *et al.*, 2007), raising the question if the anti-bacterial effect actually could be a toxic effect. To investigate the correlation between toxicity and anti-bacterial activity in this study, we also performed an *in vitro* cell toxicity assay (Section 3.13). Among the deformable liposomes, NDL showed lowest anti-bacterial effect. In most of the cases, one can see that the bacterial survival decreases with the dose, although in a small manner. This indicates that there is no significant difference in anti-bacterial effect when increasing the concentration of curcumin from 100 to 200 µg/ml. It seems that lower curcumin concentration was sufficient for the anti-bacterial effect. Moreover, curcumin, as poorly soluble molecule, can start to precipitate at higher concentrations.

**Table 7:** Anti-bacterial effect of different deformable liposomes containing curcumin expressed as bacterial survival in percentage  $\pm$  SD (n=2). \*Significantly lower than control: \*p < 0.03, \*\*p < 0.002, \*\*\*p < 0.0002, \*\*\*\*p < 0.0001. °Significantly lower than CUR-PG: °p < 0.03, °°p < 0.002, °°°p < 0.0002, °°°°p < 0.0001.

Formulation	Lipid concentration (mg/ml)	Curcumin concentration ( $\mu$ g/ml)	Bacterial survival (%)	
			<i>S. aureus</i> MSSR476	<i>S. pyogenes</i> ATCC19615
Negative control	-	-	100	100
PG sol (20%)	-	-	10.56 $\pm$ 0.24	1.87 $\pm$ 0.53
NDL	2	-	56.16 $\pm$ 2.79	2.91 $\pm$ 0.22
	4	-	63.55 $\pm$ 9.06	4.56 $\pm$ 1.06
ADL	2	-	17.88 $\pm$ 2.02	0.89 $\pm$ 0.14
	4	-	10.30 $\pm$ 0.77	0.71 $\pm$ 0.08
CDL	2	-	1.06 $\pm$ 0.01	0.20 $\pm$ 0.03
	4	-	0.79 $\pm$ 0.03	1.12 $\pm$ 0.10
CUR-PG sol	-	100	12.66 $\pm$ 0.32	1.30 $\pm$ 0.01
	-	200	12.09 $\pm$ 1.28	1.81 $\pm$ 0.44
CUR-NDL	-	100	37.93 $\pm$ 4.88***	25.33 $\pm$ 14.24**
	-	200	38.92 $\pm$ 3.48**	49.34 $\pm$ 0.88****
CUR-ADL	-	100	14.33 $\pm$ 0.63****	10.50 $\pm$ 0.28****
	-	200	9.70 $\pm$ 0.49****	8.49 $\pm$ 0.88 ****
CUR-CDL	-	100	0.19 $\pm$ 0.01 <sup>°°°°****</sup>	0.09 $\pm$ 0.01 <sup>°°°°****</sup>
	-	200	0.15 $\pm$ 0.01 <sup>°°°****</sup>	0.0 $\pm$ 0.00 <sup>°°****</sup>

#### 4.8 *In vitro* cell toxicity and proliferation assay

The topical administration of liposomes is, in general, considered to be well tolerated, however, the addition of non-phospholipid components into the liposome bilayer could attribute to the toxicity of lipid vesicles (Parnham and Wetzig, 1993). To establish the safety and toxicity of the different formulations is therefore of a great importance. In this study, a cell toxicity and proliferation assay were used to assess any potential toxic effect of the different types of deformable liposomes on human skin cells. We chose human skin fibroblasts whose

proliferation in the wound bed would contribute to wound healing (Stunova and Vistejnova, 2018). Although tests on the cell proliferation in *in vitro* condition is not directly related to the situation *in vivo*, such assays would provide important data on the activity of different formulations at the cellular level (Lappalainen *et al.*, 1994). The results of the cell proliferation assay are presented in **Figure 15**. All deformable liposomes were non-toxic to HFF cells. No cell proliferation after 12 hours for all tested formulations was observed. After 24 hours of incubation, the results showed a concentration-dependency effect, where high lipid concentration lead to a higher cell proliferation. This concentration-dependency effect was found for both empty deformable liposomes and deformable liposomes containing curcumin. Comparing to the control (untreated cells), free curcumin (Cur-PG) had little or none effect on the cell proliferation. This indicates that the effect of curcumin was enhanced when curcumin was incorporated into the deformable liposomes. Interestingly, CDL that are expected to be toxic, on the contrary, enhanced the cell proliferation.

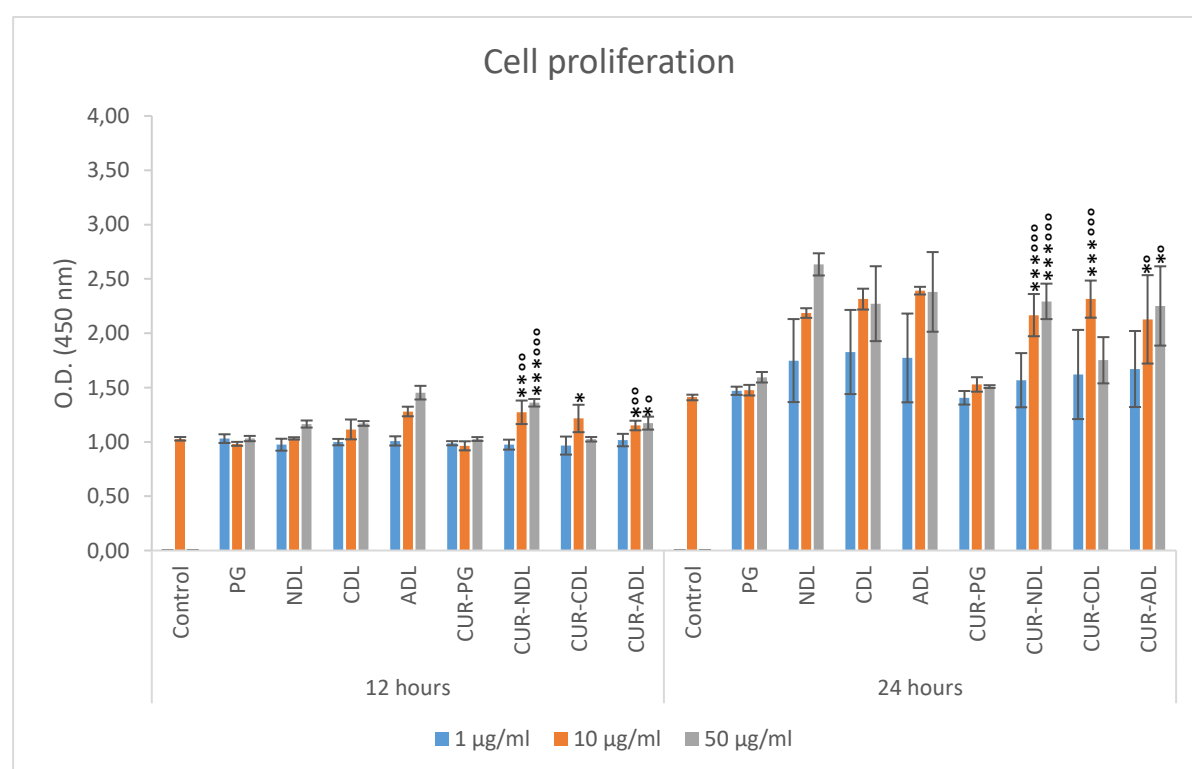


**Figure 15:** *In vitro* proliferation assay. The results are expressed as the mean optical density (O.D.) values  $\pm$  SD ( $n=3$ ) measured using CCK-8 colorimetric assay. \*Significantly different than control: \* $p < 0.03$ , \*\* $p < 0.002$ , \*\*\* $p < 0.0002$ . °Significantly different than CUR-PG: ° $p < 0.03$ , °° $p < 0.002$ , °°° $p < 0.0002$ .

It is important to notice that in this study the toxicity was assessed using only one human cell line (HFF), and it would be interesting to see if the same results could be achieved using other cell-lines as well, strengthening the results.

#### 4.9 Stability of liposomes

The shelf life of liposomes is generally determined by the physical stability that is expressed as fusion of vesicles, aggregation, and reduction in entrapment capacity (Siler-Marinkovic, 2016). Physical instability of the liposomes is expressed as the fusion/aggregation of vesicles and reduction of entrapment efficiency. After storage at 4 °C for one month, the size of the deformable liposomes was found to be similar to the original liposomal size, indicating stable liposomal formulations. The surface charge of the liposomes showed a slight decrease, and the EE seemed to be slightly affected by the storage for one month. The stability was only assessed for a one-month period, and one could hypothesize that the changes would be more significant over a longer period of storage. The result of the stability testing are presented in **Figure 16**, **Figure 17** and **Figure 18**.

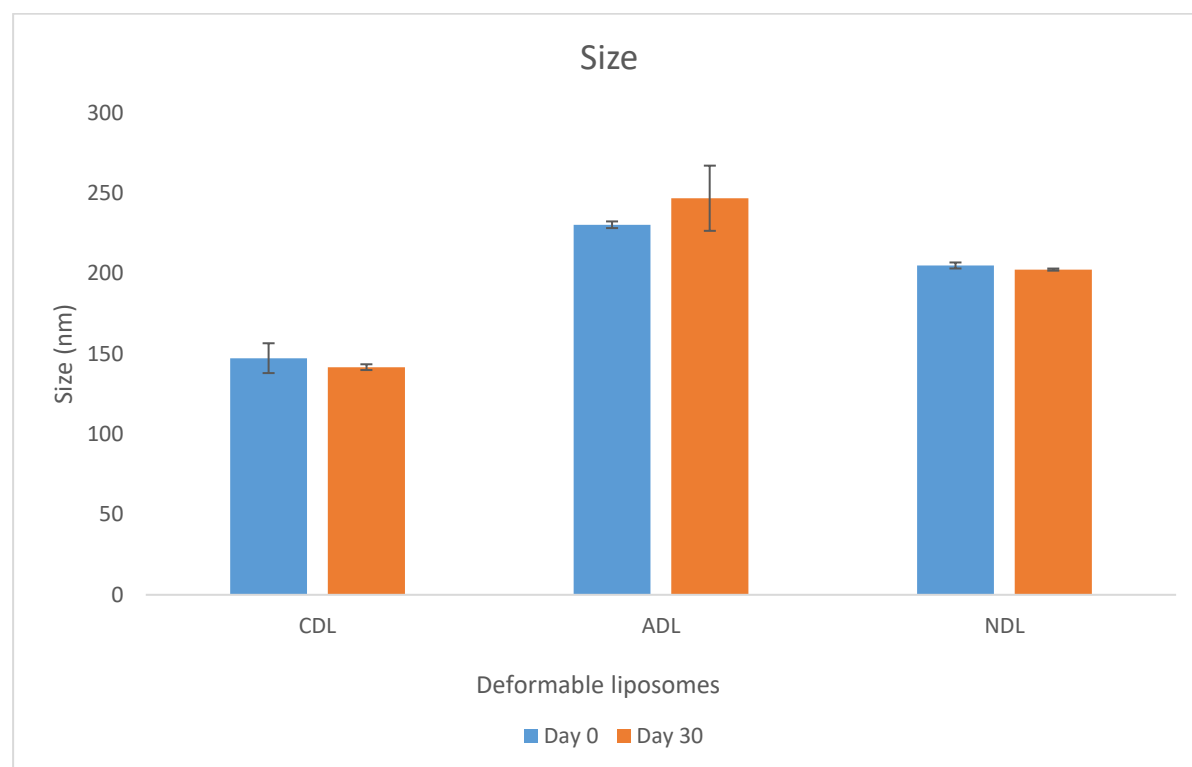


**Figure 16:** Size measurements before and after 30 days of storage at 4 °C.

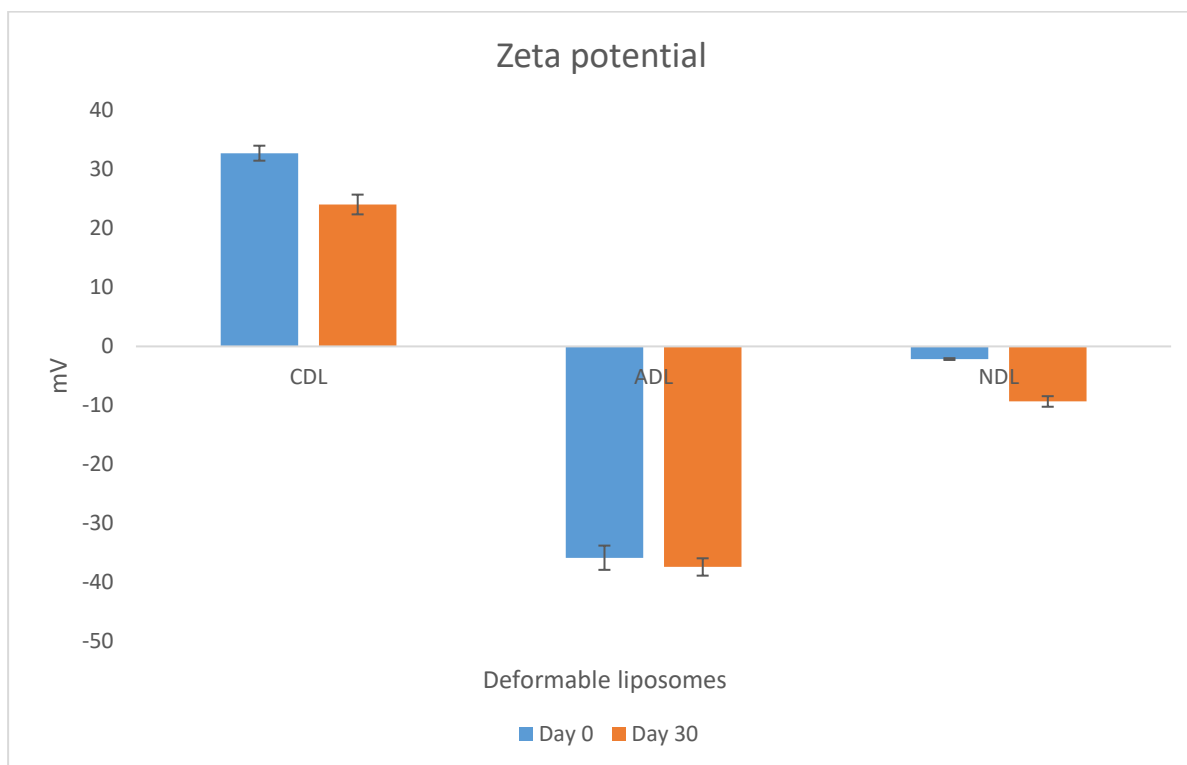


**Figure 17:** Zeta potential before and after 30 days of storage at 4 °C.

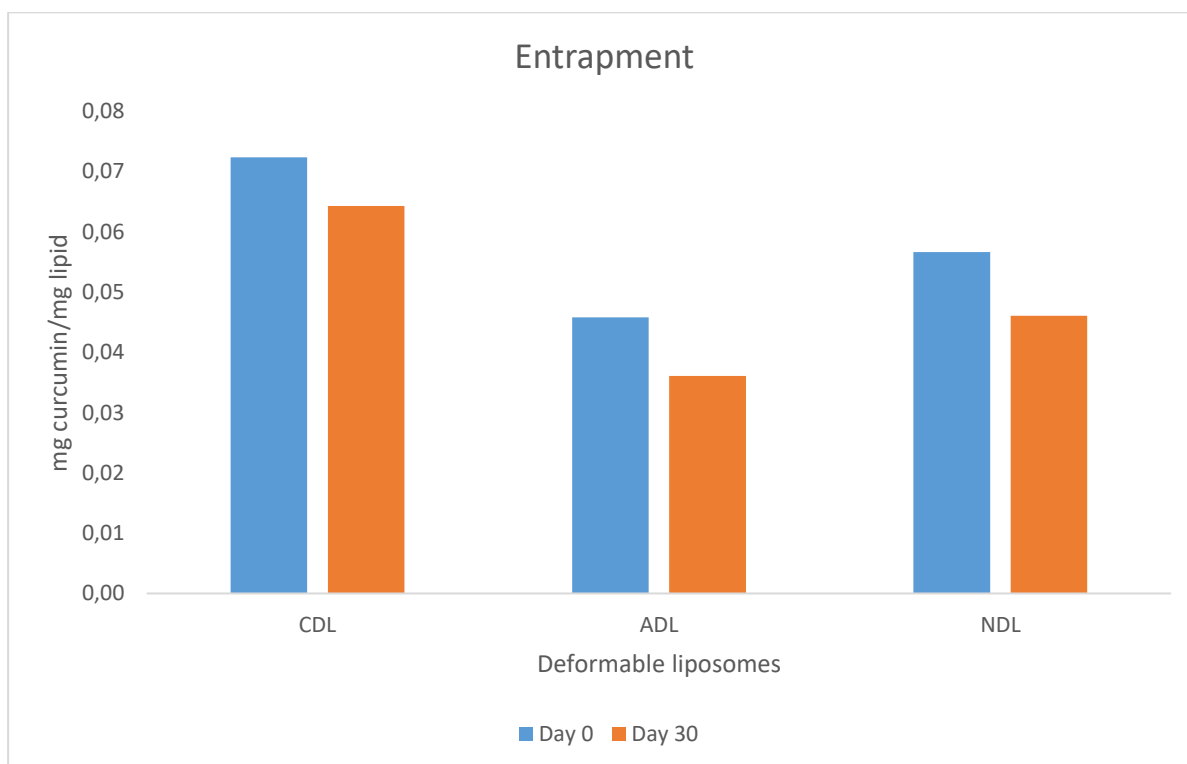


**Figure 18:** Entrapment efficiency expressed as curcumin/ lipid ratio (mg/mg) before and after 30 days of storage at 4 °C.

It would be interesting to test the stability of liposomes during the storage at room temperature or at accelerated storage conditions.

## **5 Conclusions**

In this study, the focus was on the development of deformable liposomes to improve dermal delivery of curcumin. To do so, we explored the effect of the liposomal surface charge on dermal delivery of curcumin.

The size of the deformable liposomes was optimized by the extrusion method, a simple and reproducible method, which enabled us to obtain lipid vesicles with a homogenous size distribution between 200 and 300 nm, as targeted. The zeta potential was in accordance with the surfactant used in the preparation of the liposomes, and the liposomal surface charge clearly influenced the entrapment efficiency. An effect of the liposomal surface charge was also observed for the curcumin penetration through the full thickness human skin. Cationic deformable liposomes showed a sustained curcumin penetration, which could be favorable in the treatment of chronic wounds. In addition, cationic deformable liposomes showed to enhance the anti-inflammatory and anti-bacterial activities of curcumin to a higher extent as compared to the other deformable liposomes and curcumin in solution. All liposomes were non-toxic in human skin fibroblasts and exhibited good stability after one-month storage at room temperature.

## 6 Perspectives

The deformable liposomes of different surface charge developed in this project will serve as a foundation for further optimization of dermal delivery systems containing curcumin. Based on our findings, several points need to be further exploited:

- ❖ The anti-bacterial activity of the liposomal formulations could be tested against other bacteria, possibly including Gram-negative, which are dominant in wound infections.
- ❖ The *in vitro* cell toxicity of the liposomal formulations could be tested in other types of human skin cells.
- ❖ The next step would be to incorporate the deformable liposomes into a secondary delivery vehicle such as a hydrogel. The optimization of this dual delivery system in terms of anti-inflammatory, anti-bacterial and cellular toxicity could provide further insight on the effectiveness of the novel wound dressing.
- ❖ *In vivo* animal studies and testing of the formulations in a wound model would be natural since the aim is to establish a formulation for the treatment of chronic wounds and only *in vivo* findings can confirm the proposed potential of deformable liposomes. However, it is important to consider the recommendations for limited use of laboratory animals.

## References

- Agrawal, R., Sandhu, S. K., Sharma, I. & Kaur, I. P. 2015. Development and evaluation of curcumin-loaded elastic vesicles as an effective topical anti-inflammatory formulation. *AAPS PharmSciTech*, 16, 364-374.
- Ainbinder, D., Godin, B. & Touitou, E. 2016. Ethosomes: Enhanced Delivery of Drugs to and Across the Skin. In: Dragicevic N., Maibach H. (eds) *Percutaneous Penetration Enhancers Chemical Methods in Penetration Enhancement*. Springer. Berlin, Heidelberg, 61-75.
- Akbik, D., Ghadiri, M., Chrzanowski, W. & Rohanzadeh, R. 2014. Curcumin as a wound healing agent. *Life Sciences*, 116, 1-7.
- Alexander, A., Dwivedi, S., Giri, T. K., Saraf, S., Saraf, S. & Tripathi, D. K. 2012. Approaches for breaking the barriers of drug permeation through transdermal drug delivery. *Journal of Controlled Release*, 164, 26-40.
- Ascenso, A., Salgado, A., Euletério, C., Praça, F. G., Bentley, M. V. L. B., Marques, H. C., Oliveira, H., Santos, C. & Simões, S. 2014. In vitro and in vivo topical delivery studies of tretinoin-loaded ultradeformable vesicles. *European Journal of Pharmaceutics and Biopharmaceutics*, 88, 48-55.
- Ashtikar, M. & Wacker, M. G. 2018. (In press) Nanopharmaceuticals for wound healing—Lost in translation? *Advanced Drug Delivery Reviews*.
- Balouiri, M., Sadiki, M. & Ibsouda, S. K. 2016. Methods for in vitro evaluating antimicrobial activity: A review. *Journal of Pharmaceutical Analysis*, 6, 71-79.
- Banerjee, J. & Sen, C. K. 2015. Skin Wound Healing. In: Sen, C. K. (eds) *MicroRNA in Regenerative Medicine*. Academic Press. Oxford, 631-651
- Banerjee, R. 2013. Overcoming the stratum corneum barrier: a nano approach. *Drug Delivery and Translational Research*, 3, 205-208.
- Baroli, B. 2010. Penetration of nanoparticles and nanomaterials in the skin: fiction or reality? *Journal of Pharmaceutical Sciences*, 99, 21-50.
- Barry, B. W. 1991. Modern methods of promoting drug absorption through the skin. *Molecular Aspects of Medicine*, 12, 195-241.
- Bartlett, G. R. 1959. Phosphorus assay in column chromatography. *Journal of Biological Chemistry*, 234, 466-468.
- Basnet, P., Hussain, H., Tho, I. & Skalko-Basnet, N. 2012. Liposomal delivery system enhances anti-inflammatory properties of curcumin. *Journal of Pharmaceutical Sciences*, 101, 598-609.
- Bnyan, R., Khan, I., Ehtezazi, T., Saleem, I., Gordon, S., O'neill, F. & Roberts, M. 2018. Surfactant effects on lipid-based vesicles properties. *Journal of Pharmaceutical Sciences*, 107, 1237-1246.
- Boateng, J. & Catanzano, O. 2015. Advanced therapeutic dressings for effective wound healing—a review. *Journal of Pharmaceutical Sciences*, 104, 3653-3680.
- Bozzuto, G. & Molinari, A. 2015. Liposomes as nanomedical devices. *International Journal of Nanomedicine*, 10, 975-999.
- Cevc, G. & Blume, G. 1992. Lipid vesicles penetrate into intact skin owing to the transdermal osmotic gradients and hydration force. *Biochimica et Biophysica Acta (BBA)-Biomembranes*, 1104, 226-232.
- Cevc, G. & Blume, G. 2001. New, highly efficient formulation of diclofenac for the topical, transdermal administration in ultradeformable drug carriers, Transfersomes. *Biochimica et Biophysica Acta (BBA)-Biomembranes*, 1514, 191-205.
- Dąbrowska, A., Spano, F., Derler, S., Adlhart, C., Spencer, N. & Rossi, R. 2017. The relationship between skin function, barrier properties, and body - dependent factors. *Skin Research and Technology*, 24, 165-174.
- De Leeuw, J., De Vijlder, H., Bjerring, P. & Neumann, H. 2009. Liposomes in dermatology today. *Journal of the European Academy of Dermatology and Venereology*, 23, 505-516.
- Deb, A., Mandurnekar, A. A., Rani, V., Chauhan, T., Mishra, B. & Chawla, R. 2018. Formulation and evaluation of curcumin loaded nanofilms for the treatment of wounds. *SPER Journal of Pharmaceutical and Biological Research*, 1, 5-9.

- Delouise, L. A. 2012. Applications of Nanotechnology in Dermatology. *Journal of Investigative Dermatology*, 132, 964-975.
- Dokka, S., Toledo, D., Shi, X., Castranova, V. & Rojanasakul, Y. 2000. Oxygen radical-mediated pulmonary toxicity induced by some cationic liposomes. *Pharmaceutical Research*, 17, 521-525.
- Dragicevic, N. & Maibach, H. I. 2017. *Percutaneous Penetration Enhancers Physical Methods in Penetration Enhancement*, Springer. Berlin, Heidelberg.
- Du Plessis, J., Ramachandran, C., Weiner, N. & Müller, D. 1994. The influence of particle size of liposomes on the deposition of drug into skin. *International Journal of Pharmaceutics*, 103, 277-282.
- El Zaafarany, G. M., Awad, G. a. S., Holayel, S. M. & Mortada, N. D. 2010. Role of edge activators and surface charge in developing ultradeformable vesicles with enhanced skin delivery. *International Journal of Pharmaceutics*, 397, 164-172.
- Elsayed, M., Abdallah, O. Y., Naggar, V. F. & Khalafallah, N. M. 2007a. PG - liposomes: novel lipid vesicles for skin delivery of drugs. *Journal of Pharmacy and Pharmacology*, 59, 1447-1450.
- Elsayed, M. M., Abdallah, O. Y., Naggar, V. F. & Khalafallah, N. M. 2007b. Lipid vesicles for skin delivery of drugs: reviewing three decades of research. *International Journal of Pharmaceutics*, 332, 1-16.
- Elsayed, M. M. A., Abdallah, O. Y., Naggar, V. F. & Khalafallah, N. M. 2006. Deformable liposomes and ethosomes: Mechanism of enhanced skin delivery. *International Journal of Pharmaceutics*, 322, 60-66.
- Esposito, E., Ravani, L., Mariani, P., Huang, N., Boldrini, P., Drechsler, M., Valacchi, G., Cortesi, R. & Puglia, C. 2014. Effect of nanostructured lipid vehicles on percutaneous absorption of curcumin. *European Journal of Pharmaceutics and Biopharmaceutics*, 86, 121-132.
- Flaten, G. E., Palac, Z., Engesland, A., Filipović-Grčić, J., Vanić, Ž. & Škalko-Basnet, N. 2015. In vitro skin models as a tool in optimization of drug formulation. *European Journal of Pharmaceutical Sciences*, 75, 10-24.
- Foldvari, M. & Kumar, P. 2017. Perspectives on Dermal Delivery of Macromolecular Drugs. In: Dragicevic N., Maibach H. (eds) *Percutaneous Penetration Enhancers Drug Penetration Into/Through the Skin: Methodology and General Considerations*, Springer. Berlin, Heidelberg, 355-358
- Friedrich, R. B., Kann, B., Coradini, K., Offerhaus, H. L., Beck, R. C. & Windbergs, M. 2015. Skin penetration behavior of lipid-core nanocapsules for simultaneous delivery of resveratrol and curcumin. *European Journal of Pharmaceutical Sciences*, 78, 204-213.
- Frykberg, R. G. & Banks, J. 2015. Challenges in the treatment of chronic wounds. *Advances in Wound Care*, 4, 560-582.
- Gainza, G., Pastor, M., Aguirre, J. J., Villullas, S., Pedraz, J. L., Hernandez, R. M. & Igartua, M. 2014. A novel strategy for the treatment of chronic wounds based on the topical administration of rhEGF-loaded lipid nanoparticles: in vitro bioactivity and in vivo effectiveness in healing-impaired db/db mice. *Journal of Controlled Release*, 185, 51-61.
- Gaumet, M., Vargas, A., Gurny, R. & Delie, F. 2008. Nanoparticles for drug delivery: the need for precision in reporting particle size parameters. *European Journal of Pharmaceutics and Biopharmaceutics*, 69, 1-9.
- Gillet, A., Compère, P., Lecomte, F., Hubert, P., Ducat, E., Evrard, B. & Piel, G. 2011. Liposome surface charge influence on skin penetration behaviour. *International Journal of Pharmaceutics*, 411, 223-231.
- González-Rodríguez, M. L., Cózar-Bernal, M. J., Fini, A. & Rabasco, A. M. 2016. Surface-Charged Vesicles for Penetration Enhancement. *Percutaneous Penetration Enhancers Chemical Methods in Penetration Enhancement*. Springer. Berlin, Heidelberg, 121-136.
- Grimaldi, N., Andrade, F., Segovia, N., Ferrer-Tasies, L., Sala, S., Veciana, J. & Ventosa, N. 2016. Lipid-based nanovesicles for nanomedicine. *Chemical Society Reviews*, 45, 6520-6545.
- Hua, S. 2015. Lipid-based nano-delivery systems for skin delivery of drugs and bioactives. *Frontiers in Pharmacology*, 6, 219.

- Hussain, Z., Thu, H. E., Ng, S.-F., Khan, S. & Katas, H. 2017. Nanoencapsulation, an efficient and promising approach to maximize wound healing efficacy of curcumin: A review of new trends and state-of-the-art. *Colloids and Surfaces B: Biointerfaces*, 150, 223-241.
- Ita, K. B. 2014. Transdermal drug delivery: progress and challenges. *Journal of Drug Delivery Science and Technology*, 24, 245-250.
- Jain, S., Jain, P., Umamaheshwari, R. & Jain, N. 2003. Transfersomes—a novel vesicular carrier for enhanced transdermal delivery: development, characterization, and performance evaluation. *Drug Development and Industrial Pharmacy*, 29, 1013-1026.
- Janis, J. & Attinger, C. 2006. The basic science of wound healing. *Plastic and Reconstructive Surgery*, 117, 12S-34S.
- Kotla, N. G., Chandrasekar, B., Rooney, P., Sivaraman, G., Larrañaga, A., Krishna, K. V., Pandit, A. & Rochev, Y. 2017. Biomimetic lipid-based nanosystems for enhanced dermal delivery of drugs and bioactive agents. *ACS Biomaterials Science & Engineering*, 3, 1262-1272.
- Krausz, A. E., Adler, B. L., Cabral, V., Navati, M., Doerner, J., Charafeddine, R. A., Chandra, D., Liang, H., Gunther, L. & Clendaniel, A. 2015. Curcumin-encapsulated nanoparticles as innovative antimicrobial and wound healing agent. *Nanomedicine: Nanotechnology, Biology and Medicine*, 11, 195-206.
- Lai-Cheong, J. E. & McGrath, J. A. 2017. Structure and function of skin, hair and nails. *Medicine*, 45, 347-351.
- Lane, M. E. 2013. Skin penetration enhancers. *International Journal of Pharmaceutics*, 447, 12-21.
- Lappalainen, K., Jääskeläinen, I., Syrjänen, K., Urtti, A. & Syrjänen, S. 1994. Comparison of cell proliferation and toxicity assays using two cationic liposomes. *Pharmaceutical Research*, 11, 1127-1131.
- Lee, T. & Friedman, A. 2016. Skin Barrier Health: Regulation and Repair of the Stratum Corneum and the Role of Over-the-Counter Skin Care. *Journal of Drugs in Dermatology*, 15, 1047-1051.
- Li, J., Chen, J. & Kirsner, R. 2007. Pathophysiology of acute wound healing. *Clinics in Dermatology*, 25, 9-18.
- Maestrelli, F., González-Rodríguez, M. L., Rabasco, A. M., Ghelardini, C. & Mura, P. 2010. New “drug-in cyclodextrin-in deformable liposomes” formulations to improve the therapeutic efficacy of local anaesthetics. *International Journal of Pharmaceutics*, 395, 222-231.
- Mehanny, M., Hathout, R. M., Geneidi, A. S. & Mansour, S. 2016. Exploring the use of nanocarrier systems to deliver the magical molecule; curcumin and its derivatives. *Journal of Controlled Release*, 225, 1-30.
- Menon, G. K. 2015. Skin basics; structure and function. In: Pappas A.(eds) *Lipids and Skin Health*. Springer, Cham, 9-23.
- Mohanty, C. & Sahoo, S. K. 2017. Curcumin and its topical formulations for wound healing applications. *Drug Discovery Today*, 22, 1582-1592.
- Morton, L. M. & Phillips, T. J. 2016. Wound healing and treating wounds: Differential diagnosis and evaluation of chronic wounds. *Journal of the American Academy of Dermatology*, 74, 589-605.
- Moser, K., Kriwet, K., Naik, A., Kalia, Y. N. & Guy, R. H. 2001. Passive skin penetration enhancement and its quantification in vitro. *European Journal of Pharmaceutics and Biopharmaceutics*, 52, 103-112.
- Mota, A. H., Rijo, P., Molpeceres, J. & Reis, C. P. 2017. Broad overview of engineering of functional nanosystems for skin delivery. *International Journal of Pharmaceutics*, 532, 710-728.
- Ng, K. W. & Lau, W. M. 2015. Skin deep: the basics of human skin structure and drug penetration. In: Dragicevic N., Maibach H. (eds) *Percutaneous Penetration Enhancers Chemical Methods in Penetration Enhancement*. Springer, Berlin, Heidelberg, 3-11.
- Ogiso, T., Yamaguchi, T., Iwaki, M., Tanino, T. & Miyake, Y. 2001. Effect of positively and negatively charged liposomes on skin permeation of drugs. *Journal of Drug Targeting*, 9, 49-59.
- Palac, Z., Hurler, J., Škalko-Basnet, N., Filipović-Grčić, J. & Vanić, Ž. 2015. Elastic liposomes-in-vehicle formulations destined for skin therapy: the synergy between type of liposomes and vehicle. *Drug Development and Industrial Pharmacy*, 41, 1247-1253.

- Parnham, M. J. & Wetzig, H. 1993. Toxicity screening of liposomes. *Chemistry and Physics of Lipids*, 64, 263-274.
- Prow, T. W., Grice, J. E., Lin, L. L., Faye, R., Butler, M., Becker, W., Wurm, E. M., Yoong, C., Robertson, T. A. & Soyer, H. P. 2011. Nanoparticles and microparticles for skin drug delivery. *Advanced Drug Delivery Reviews*, 63, 470-491.
- Rakesh, R. & Anoop, K. 2012. Ethosomes for transdermal and topical drug delivery. *International Journal of Pharmacy and Pharmaceutical Sciences*, 4, 17-24.
- Riehemann, K., Schneider, S. W., Luger, T. A., Godin, B., Ferrari, M. & Fuchs, H. 2009. Nanomedicine—challenge and perspectives. *Angewandte Chemie International Edition*, 48, 872-897.
- Rodrigues, J., Prather, K. L., Kluskens, L. & Rodrigues, L. 2015. Heterologous production of curcuminoids. *Microbiology and Molecular Biology Reviews*, 79, 39-60.
- Rukavina, Z. & Vanić, Ž. 2016. Current trends in development of liposomes for targeting bacterial biofilms. *Pharmaceutics*, 8, 18.
- Sala, M., Diab, R., Elaissari, A. & Fessi, H. 2018. Lipid nanocarriers as skin drug delivery systems: Properties, mechanisms of skin interactions and medical applications. *International Journal of Pharmaceutics*, 535, 1-17.
- Satyam, G., Shivani, S. & Garima, G. 2015. Ethosomes: A novel tool for drug delivery through the skin. *Journal of Pharmacy Research*, 3, 688-691.
- Siler-Marinkovic, S. 2016. Liposomes as Drug Delivery Systems in Dermal and Transdermal Drug Delivery. In: Dragicevic N., Maibach H. (eds) *Percutaneous Penetration Enhancers Chemical Methods in Penetration Enhancement*. Springer. Berlin, Heidelberg, 15-38.
- Simões, D., Miguel, S. P., Ribeiro, M. P., Coutinho, P., Mendonça, A. G. & Correia, I. J. 2018. Recent advances on antimicrobial wound dressing: A review. *European Journal of Pharmaceutics and Biopharmaceutics*, 127, 130-141.
- Smistad, G., Jacobsen, J. & Sande, S. A. 2007. Multivariate toxicity screening of liposomal formulations on a human buccal cell line. *International Journal of Pharmaceutics*, 330, 14-22.
- Stadelmann, W. K., Digenis, A. G. & Tobin, G. R. 1998. Physiology and healing dynamics of chronic cutaneous wounds. *The American Journal of Surgery*, 176, 26S-38S.
- Stunova, A. & Vistejnova, L. 2018. Dermal fibroblasts—A heterogeneous population with regulatory function in wound healing. *Cytokine & growth factor reviews*, 39, 137-150.
- Suwannateep, N., Wanichwecharungruang, S., Haag, S., Devahastin, S., Groth, N., Fluhr, J., Lademann, J. & Meinke, M. 2012. Encapsulated curcumin results in prolonged curcumin activity in vitro and radical scavenging activity ex vivo on skin after UVB-irradiation. *European Journal of Pharmaceutics and Biopharmaceutics*, 82, 485-490.
- Ternullo, S., De Weerd, L., Holsæter, A. M., Flaten, G. E. & Škalko-Basnet, N. 2017. Going skin deep: A direct comparison of penetration potential of lipid-based nanovesicles on the isolated perfused human skin flap model. *European Journal of Pharmaceutics and Biopharmaceutics*, 121, 14-23.
- Thapa, B., Pepic, I., Vanic, Z., Basnet, P. & Skalko-Basnet, N. 2013. Topical delivery system for phytochemicals: capsaicin and capsicum tincture. *Journal of Pharmaceutics & Drug Development*, 1, 1-7.
- Van Smeden, J., Janssens, M., Gooris, G. S. & Bouwstra, J. A. 2014. The important role of stratum corneum lipids for the cutaneous barrier function. *Biochimica et Biophysica Acta (BBA) - Molecular and Cell Biology of Lipids*, 1841, 295-313.
- Vanić, Ž., Hurler, J., Ferderber, K., Golja Gašparović, P., Škalko-Basnet, N. & Filipović-Grčić, J. 2014. Novel vaginal drug delivery system: deformable propylene glycol liposomes-in-hydrogel. *Journal of Liposome Research*, 24, 27-36.
- Wenkers, B. P. & Lippold, B. C. 1999. Skin penetration of nonsteroidal antiinflammatory drugs out of a lipophilic vehicle: influence of the viable epidermis. *Journal of Pharmaceutical Sciences*, 88, 1326-1331.
- Wernick, B. & Stawicki, S. 2018. Wound, Impaired Healing. In: StatPearls [Internet]. Treasure Island (FL): StatPearls Publishing. Available from: <https://europepmc.org/books/NBK482254>

Zhao, Y.-Z., Lu, C.-T., Zhang, Y., Xiao, J., Zhao, Y.-P., Tian, J.-L., Xu, Y.-Y., Feng, Z.-G. & Xu, C.-Y. 2013. Selection of high efficient transdermal lipid vesicle for curcumin skin delivery. *International Journal of Pharmaceutics*, 454, 302-309.

